Indefinite Causal Orders in Thermodynamics and from Time Superpositions



David Felce

Merton College

University of Oxford

A thesis submitted for the degree of

Doctor of Philosophy

Michaelmas 2021

Acknowledgements

It is impossible to imagine that this thesis could have been completed without the kind and patient help and encouragement of many colleagues, friends, and family members. First, I would like to thank my supervisor, Vlatko Vedral. His insights and advice have been indispensable at every stage of the project. I am also grateful for the way in which he gave me a home in his group, after an unexpected departure from my previous one, during the second year of my studies. I also thank my first supervisor, Ian Walmsley, for bringing me to Oxford. My gratitude is owed to the British taxpayer (EPSRC) and M Squared Lasers Limited for funding this research.

I have been very fortunate to share my time in the Frontiers of Quantum Physics group with many brilliant and genuine people, all of whom have helped me in some way or another. Felix Tennie has been a great collaborator and guide on a wide range of matters, and I wish to thank him for our many games of chess over the board and online! I shared another very fruitful and enjoyable collaboration with Eduardo Dias and Nicetu Tibal Vidal. I will fondly remember our fiery Zoom meetings! I thank Benjamin Yadin for many probing and clarifying comments at crucial junctures throughout this research process. There were many others who contributed to this work through countless conversations and debates, not least Aditya Iyer, Sam Kuypers, and Jinzhao Sun, who kept me very entertained for the period when the office was open and during our adventures in Singapore! I would also like to thank Adrian Menssen, for welcoming me into my first group as a mentor, and remaining a good friend. I look forward to the day when we can pay Dr. Pepper another visit together.

I would like to thank my parents and siblings for instilling in me a curiosity about the big questions. Together with my wife's family, I thank them for their loving support and encouragement, and for always giving us homes on both sides of the Atlantic. Finally, I would like to thank my wife Abigail and our son Simeon. Abigail, thank you for sticking by me and loving me through the good times and the bad, and for pushing me over the line when I really needed it. You are my greatest earthly treasure. Simeon, thank you for keeping things fun. I dedicate this thesis to you.

Chiefly, I wish to give humble thanks to almighty God, who 'looking upon [me] in His Son, is pleased to accept and reward that which is sincere, although accompanied with many weaknesses and imperfections.'[1]

[1] Westminster Confession of Faith 16.6

Abstract

This thesis is concerned with the use of indefinite causal orders (ICOs) for thermodynamic tasks, and a new context in which these exotic causal structures might arise — from superpositions in time. I propose a thermodynamic refrigeration cycle which uses indefinite causal orders to achieve non-classical cooling. The cycle cools a cold reservoir while consuming purity in a control qubit. I first show that the application to an input state of two identical thermalising channels of temperature T in an indefinite causal order can result in an output state with a temperature not equal to T. This result allows the construction of the refrigeration cycle. I investigate its properties and show that thermodynamically, the result is compatible with unitary quantum mechanics in the circuit model, but could not be achieved classically. This result suggests the development of a new class of thermodynamic resource theories in which operations are allowed to be performed in an indefinite causal order. I proceed to detail a simulation of the protocol using the IBM cloud quantum computing service, which is open to all users of the internet. The simulation, which is itself a quantum refrigerator, shows that the refrigeration cycle is robust to noise and can be implemented on Noisy Intermediate-Scale Quantum (NISQ) devices. This represents the development of a promising new test-bed for ICO protocols. Finally, the possibility for ICOs to arise from superpositions in time is considered. A new formalism, developed to analyse such superpositions, is applied to the case of two events which have a quantum uncertainty associated with their times. It is shown that these events can be used as triggers which enable an ICO. The fact that such commonplace phenomena can give rise to indefinite causal orders suggests that they might be much more common in nature than is typically understood.

Contents

1 Introduction **1**

1.1 Basic Overview 1

1.2 The Channel Picture in Quantum Mechanics 5

1.2.1 Unitary Evolution 5

1.2.2 Density Operators 7

1.2.3 Quantum Channels 8

1.3 Indefinite Causal Orders 10

1.3.1 Causal Orders for Closed Laboratories 10

1.3.2 The Quantum SWITCH 14

1.3.3 Physical Realisation 16

1.3.4 Applications 17

2 Quantum Refrigeration with Indefinite Causal Order **19**

2.1 Thermalising Channels in an Indefinite Causal Order— 19

2.2 Simulation Quantum Circuit 22

2.3 ICO Refrigerator 23

2.3.1 Two-level Refrigeration Cycle 24

2.3.2 Three-level Refrigeration Cycle 27

2.4 Performance of the Refrigerators 28

2.4.1 Two-level Refrigerator Performance 28

2.4.2 Three-level Refrigerator Performance 32

2.5 Discussion 34

3 Cloud Quantum Refrigeration **37**

3.1 Introduction 37

3.2 Methods 40

3.3 Results 42

3.4 Noise Considerations 44

3.5 Future Circuits 46

3.6 Discussion 48

4 Indefinite Causal Order from Superpositions in Time 51
4.1 Introduction 52
4.2 Formalism for Quantum Events 53
4.3 Deriving ICO from Superpositions in Time 55
4.4 Strategies for a Quantum SWITCH via Time Superpositions 59
4.4.1 Via Time-Bin Entanglement 59
4.4.2 Via Decaying Atoms 60
4.4.3 Alternative Derivation for Decaying Atoms protocol 61
4.5 Discussion 64

5 Summary and Further Work 69
5.1 Summary of Research Findings 69
5.2 Avenues for Further Investigation 71

Appendices

A Supplementary Materials - Cloud Quantum Refrigerator 75
A.1 Quantum Circuit Output Calculation 75
A.2 IBMq Transpiled Circuit 78

References 83

We possess scientific knowledge of a thing only when we know its cause...

—Aristotle's *Posterior Analytics*

1 Introduction

Contents

1.1 Basic Overview 1
1.2 The Channel Picture in Quantum Mechanics 5
1.2.1 Unitary Evolution 5
1.2.2 Density Operators 7
1.2.3 Quantum Channels 8
1.3 Indefinite Causal Orders 10
1.3.1 Causal Orders for Closed Laboratories 10
1.3.2 The Quantum SWITCH 14
1.3.3 Physical Realisation 16
1.3.4 Applications 17

1.1 Basic Overview

Causality has always been at the heart of human understanding of the world. The laws of cause and effect govern our daily lives, and seem so intuitive to us that we take their operation for granted. The concept of causality plays a long and important role in the history of Physics. In the first recorded work of Physics, Aristotle's *Physics*, written in the 4^{th} century BC, the four causes (material, efficient, formal, and final) play a central role in understanding the natural world. The classical Physics of Galileo and Newton enable a quantitative understanding of the causes of

the motions of objects, in terms of the forces which act on them. These developments made possible a general framework of cause and effect which claimed to explain all of physical reality. Einstein's special and general theories of relativity transformed our understanding of space and time in very counter-intuitive ways, showing, for example, that whether two events are simultaneous is an observer-dependent fact. However, causality remained a crucial concept in the new framework. The theory of special relativity places a limit on how fast light, and therefore information can travel. This defines an observer-independent causal past and causal future for each event, giving rise to a fixed causal relationship between these events.

as well as the ability of an event in the past to cause an event in the future,

But it is the quantum mechanical revolution that has transformed our understanding of causality in the most fundamental way since Aristotle. Although the equations which govern the evolution of quantum systems are deterministic, when an observer makes measurements on such a system, sometimes the results he obtains will be distributed randomly. This randomness poses problems for any system of universal causation, in which every event has a cause. After all, if a measurement is truly random then it is impossible to answer the question of what caused a certain measurement result, when another result was just as likely. When it comes to describing the experiences of an observer, quantum mechanics lacks a complete framework of causality.

Another counter-intuitive aspect of causality in quantum mechanics, which will be the focus of this thesis, is the possibility for events to take place in a superposition of causal orders. In the classical picture, there is one absolute order in which all events in the universe take place. Even in the relativistic picture, where the time of an event depends on its observer, events which can causally influence one another have a fixed order for all observers (they are time-like separated). In quantum mechanics however, it is not disallowed that operations are applied to a system in a superposition of different orders, just as a particle can be located at a superposition of different positions. Thus, a situation can arise in which events that are causally linked have an order which is not well-defined classically.

It can be shown that the effects of two or more operations applied in such an indefinite causal order are very surprising, differing dramatically from those of the operations applied individually or in any classical order. One example is a recent work in which it was shown that two communication channels which are ordinarily completely useless — noisy channels which replace the input state with a completely random state — can become useful when applied in an indefinite causal order. If the receiver of the output state is allowed access to a control qubit which is correlated with the quantum order in which the noisy operations are performed, then he will be able to extract some information about the input state. In other words, communication channels which can normally transmit no information are able to do so, when applied in an indefinite causal order.

These exotic causal structures, and their surprising usefulness in thermodynamics (the science of work and heat), are the subject of this thesis. In the first main chapter, a novel approach to quantum refrigeration is developed, which relies upon indefinite causal orders. The protocol relies on a strange property of thermalising operations in an indefinite causal order. A thermalising operation ordinarily has a very simple outcome; the output state does not depend at all on the input state, but is always the same random state with a certain temperature (temperature β, for instance). When these operations are applied in an indefinite causal order the resulting state is very different. In this case, the output state retains a dependence on the input state, and, most surprisingly, the output state in general will not have the same temperature (β), which is the normal output temperature of the operation.

In everyday terms, a thermalising operation can be imagined as the placing of a cup of tea inside a bathtub full of water. After some time has elapsed, the tea inside the cup will be at the same temperature as the water in the bath. Of course, if we repeat this experiment with two baths (A and B), both filled with water at the same temperature, the outcome will be the same. Whether we place the cup into bath A first, and then into bath B, or vice versa, the tea will finish at the common temperature of the baths. The results of this thesis indicate however, that if we were able to place these operations in a quantum superposition of orders,

placing the cup into bath A first then into bath B, *and* placing the cup into bath B first then into bath A, at the end of the process, the tea in the cup would have a different temperature to the water in the bathtubs.

The strange properties of thermalising channels, when placed in an indefinite causal order, enable the construction of a refrigeration cycle, which transfers heat from a colder reservoir to a hotter reservoir, and whose only energy cost is that of performing a measurement. This cycle is explained and analysed in the chapter 2 of this thesis.

A version of the refrigeration protocol can be run on a quantum computer. In the chapter 3 the implementation of the protocol on an *IBM Quantum* cloud quantum computer is described. Quantum bits of this computer are shown to have been cooled, providing proof of principle of the Indefinite Causal Order quantum refrigerator. This demonstration is achieved using resources available to all users of the internet.

The experimental implementation of the refrigerator allows the robustness of the refrigeration protocol to be tested. It is verified that refrigeration can be achieved using a noisy platform, which is encouraging for the future applicability of the protocol in various systems.

At the time of writing, there is a degree of controversy about the physical situations in which an indefinite causal order might arise. Some argue that only a theory of quantum gravity, in which the fabric of space-time can be in a superposition of configurations, could describe a scenario in which indefinite causal orders are present. In chapter 4, the possibility of indefinite causal orders arising from quantum superpositions in time, without the need for complicated theories of quantum gravity, is discussed.

There are phenomena which are naturally 'fuzzy' in time in quantum mechanics, such as the decay of an excited atom. The atom must decay at some point, but there is no deterministic way to predict the particular time when this event will occur. Instead, at each time, the atom can be considered to be in a superposition of not-decayed and already-decayed states. A novel formalism is used to treat the time of the decay of the atom as a quantum variable, which is itself in a superposition.

We proceed to examine the situation of two excited atoms ready to decay. Each atom is connected to a machine in such a way that its decay triggers the operation of the machine on a target system. Because the time of decay of both atoms is in a superposition, the operations trigger in an indefinite causal order. When atom A decays first then operation A triggers first and then operation B. When atom B decays first then the operations take place in the opposite order. The result is a quantum superposition of orders of the operations.

As well as developing a theoretical description of how indefinite causal orders might arise from superpositions in time, we propose two specific physical implementations of the protocol, using decaying atoms, as discussed above, and using photons which are entangled in time. That indefinite causal orders can arise simply from processes which are 'fuzzy' in time, which occur commonly in nature, implies that they themselves may be more common in nature than previously imagined. It is even possible that there are phenomena in nature which can only be explained with reference to indefinite causal orders. We now proceed to lay some of the conceptual foundation necessary for the results which follow.

1.2 The Channel Picture in Quantum Mechanics

1.2.1 Unitary Evolution

In quantum mechanics, the evolution of an isolated system is governed by the Schrödinger equation [1]:

$$i\hbar\frac{\partial}{\partial t}\left|\psi(t)\right\rangle = \hat{H}\left|\psi(t)\right\rangle, \tag{1.1}$$

where $|\psi(t)\rangle$ is the vector in Hilbert space representing the quantum state at the instant of time t, and $\hat{H}$ is the Hamiltonian operator, corresponding to the energy of the system. This linear differential equation can be solved to give the value of $|\psi(t)\rangle$ for all times, with the solution being

$$\left|\psi(t)\right\rangle = e^{-i\hat{H}t/\hbar}\left|\psi(0)\right\rangle, \tag{1.2}$$

Here $|\psi(0)\rangle$ represents the initial state of the quantum system. The time evolution operator $e^{-i\hat{H}t/\hbar}$ is unitary, so we write

$$|\psi(t)\rangle = \hat{U}(t)\,|\psi(0)\rangle\,. \tag{1.3}$$

This statement of the equation of motion explicitly demonstrates that the full evolution of an isolated system under the laws of quantum mechanics is unitary.

However, when we consider subsystems which are interacting with their environment, further refinements are necessary. It is not true in general that the evolution of subspaces of the full Hilbert space is unitary. To see this, let us consider the action of a unitary operator on a bipartite system which begins in a product state $|\psi(0)\rangle = |\phi_A(0)\rangle_A \otimes |\phi_B(0)\rangle_B$. In this initial product state, there is no entanglement between subsystems A and B, and each can be fully described without reference to the other. The time-evolved state is then given by

$$|\psi(t)\rangle = \hat{U}(t)\ \ |\phi_A(0)\rangle_A \otimes |\phi_B(0)\rangle_B\,. \tag{1.4}$$

In some cases, the total unitary $\hat{U}(t)$ can be decomposed into two components so that it becomes $\hat{U}_A(t)\otimes\hat{U}_B(t)$, where $\hat{U}_A(t)$ and $\hat{U}_B(t)$ operate on the Hilbert subspaces A and B respectively. In this case, each subsystem separately obeys the time-evolution equation (1.3). However, in the general case in which this decomposition is not possible, the evolution of each subspace is non-unitary. If an observer is restricted to one of these subspaces, he will therefore require a new formalism to describe the evolution which he observes. Furthermore, in general, the state of the full system $|\psi(t)\rangle$ will no longer be able to be written as a product state on the two subspaces A and B. As a result, an observer with access to only one subsystem will no longer be able to describe this subsystem with a vector in his Hilbert subspace. Such an observer will need a new mathematical object to describe the states that he observes.

1.2.2 Density Operators

The density operator [2] is a more general representation of the state of a quantum system which can be used even when this state has an uncertainty associated with it. Mathematically, it is a positive semi-definite, Hermitian operator on the Hilbert space, with unit trace. This operator admits the decomposition

$$\hat{\rho} = \sum_i p_i \left|\psi_i\right\rangle \left\langle\psi_i\right| . \tag{1.5}$$

This is the density operator for a system which is prepared in the pure quantum state $|\psi_i\rangle$, with probability p_i. Each probability p_i must be positive and the set of all probabilities must sum to unity. Thus constructed, it is easy to see that the time-evolution of the density operator of a closed system is given by

$$\hat{\rho}(t) = \sum_i p_i \hat{U}(t) \left|\psi_i(0)\right\rangle \left\langle\psi_i(0)\right| \hat{U}(t)^\dagger = \hat{U}(t)\hat{\rho}(0)\hat{U}(t)^\dagger, \tag{1.6}$$

since this represents the unitary evolution of equation (1.3) applied to each of the possible pure states of the system.

Let us return to the bipartite system considered above. The initial product state can be written

$$\hat{\rho}_{AB}(0) = \hat{\rho}_A(0) \otimes \hat{\rho}_B(0), \tag{1.7}$$

with $\hat{\rho}_A(0) = \left|\phi_A(0)\right\rangle_A \left\langle\phi_A(0)\right|_A$ and $\hat{\rho}_B(0) = \left|\phi_B(0)\right\rangle_B \left\langle\phi_B(0)\right|_B$. The state after time t then becomes

$$\hat{\rho}_{AB}(t) = \hat{U}(t)\hat{\rho}_A(0) \otimes \hat{\rho}_B(0)\hat{U}^\dagger(t). \tag{1.8}$$

It is now possible to describe the state of a single subsystem using the density operator formalism. The reduced density operator of subsystem A, which contains all information about this subsystem which is available without reference to B, is defined via the partial trace

$$\hat{\rho}_A \equiv \mathrm{Tr}_B(\hat{\rho}_{AB}). \tag{1.9}$$

For a general state on two subsystems A and B (expanded in basis states $|\psi_i\rangle_A$ and $|\phi_i\rangle_B$)

$$\Psi_{AB} = \sum_{ijkl} c_{ijkl} \, |\psi_i\rangle \langle\psi_j|_A \otimes |\phi_k\rangle \langle\phi_l|_B \, , \tag{1.10}$$

where c_{ijkl} are complex coefficients. The partial trace superoperator Tr_B is itself defined by

$$\mathrm{Tr}_B\Big(\Psi_{AB}\Big) \equiv \sum_{ijkl} c_{ijkl} \, |\psi_i\rangle \langle\psi_j|_A \;\; \mathrm{Tr}\Big(|\phi_k\rangle \langle\phi_l|_B \Big), \tag{1.11}$$

where $\mathrm{Tr}\Big(|\phi_k\rangle_B \langle\phi_l|_B \Big) = \langle\phi_l|\phi_k\rangle_B$ is the ordinary trace operation. This relation can also be written

$$\mathrm{Tr}_B\Big(\Psi_{AB}\Big) \equiv \sum_i (\mathbb{I}_A \otimes \langle b_i|_B) \Psi_{AB} (\mathbb{I}_A \otimes |b_i\rangle_B), \tag{1.12}$$

where $\mathbb{I}_A$ is the identity on Hilbert subspace A, and the set $\{|b_i\rangle_B\}$ forms a basis for Hilbert subspace B.

It can be shown that the definition of the reduced density operator yields the correct measurement statistics (the measurement probabilities for an observable on the subspace are identical whether calculated from the full state or the reduced density operator), and is thus a good representation of the knowledge about the state of a subsystem that an observer restricted to its subspace can possess. The density operator formalism thus enables us to describe quantum systems which are interacting with their environment and whose state is subject to a degree of uncertainty. It is to the evolution of such systems that we now turn.

1.2.3 Quantum Channels

The generalisation of the Schrödinger equation for open quantum systems is given in the quantum channel picture by

$$\rho(t) = \mathcal{N}(t)[\rho(0)], \tag{1.13}$$

which replaces equation (1.3) from the pure state vector formalism (from this point we suppress the operator hat notation, e.g. $\hat{\rho}$, to simplify notation). The quantum channel $\mathcal{N}$ takes the mathematical form of a completely positive trace-preserving (CPTP) map. These properties ensure that a quantum channel always maps a valid density operator onto another valid density operator. A quantum channel acting on a system can always be represented by a unitary operation acting on the system plus an environment. Such a representation is called the unitary extension of the channel:

$$\mathcal{N}[\rho_S] = \mathrm{Tr}_E\Big(U_{SE}[\rho_S \otimes |0\rangle\langle 0|_E]U_{SE}^\dagger\Big). \tag{1.14}$$

Here U_{SE} is the unitary extension of the channel and acts on the joint space of the system and environment $S \otimes E$. The initial state of the environment is labelled $|0\rangle\langle 0|_E$, and is chosen to be a pure state for the sake of simplicity. The fact that any quantum channel can be written in this way is known as Stinespring's dilation theorem [3]. From this relation follows a decomposition for quantum channels which will be of particular utility in what follows. Writing out the partial trace in terms of basis states of the environment $|i\rangle_E$ according to equation (1.12), we have

$$\mathcal{N}[\rho_S] = \sum_i (\mathbb{I}_S \otimes \langle i|_E)\Big(U_{SE}[\rho_S \otimes |0\rangle\langle 0|_E]U_{SE}^\dagger\Big)(\mathbb{I}_S \otimes |i\rangle_E), \tag{1.15}$$

which can be manipulated to give

$$\mathcal{N}[\rho_S] = \sum_i K_i \rho_S K_i^\dagger. \tag{1.16}$$

This is known as the Kraus decomposition of the quantum channel, whose Kraus operators are defined by

$$K_i = \langle i|_E U_{SE} |0\rangle_E . \tag{1.17}$$

The Kraus operators satisfy the completeness relation

$$\sum_i K_i^\dagger K_i = \mathbb{I}, \tag{1.18}$$

which ensures that any quantum channel constructed via equation (1.16) is trace preserving.

Now that we have the mathematical tools in place, we turn to the phenomenon which will be central to each part of this thesis, that of Indefinite Causal Orders (ICOs).

1.3 Indefinite Causal Orders

1.3.1 Causal Orders for Closed Laboratories

The existence of a fixed causal structure underlying events that take place is a feature of all of classical and most of quantum physics. In the field of Quantum Information this is most recognisable when one considers the quantum circuit formalism. In a quantum circuit, the causal relationship between each gate is fixed — determined by the configuration of the wires which connect them. The output of each gate is connected to the input of the next in a straightforward way, and there can be no loops, since this would represent information travelling back in time.

More recently, however, a body of work (e.g. Refs. [4–8]) has arisen concerning situations in which the causal order is not fixed. In these cases, unlike in a quantum circuit, it is not possible to assign a definite causal relationship between the events or operations which occur. These situations are said to exhibit indefinite causal order. One particular context in which more interesting causal structures may be considered is that of experimenters who are located in laboratories which are closed, that is, they are isolated from any events happening outside their laboratories. The only exception to this is that each laboratory is opened once to allow a quantum system (perhaps a spin-$\frac{1}{2}$ particle) to enter, and once to allow this system to leave. While the system is inside each laboratory, the experimenter may perform operations, including measurements, on it. Inside each laboratory the causal order is fixed, but the causal relationship between each laboratory need not be so.

Let us consider a situation in which there are two experimenters, Alice and Bob, each inside their own closed laboratory. This is the same situation as that considered in [5], and what follows is a summary of the main result of that paper.

A certain communication task is given to Alice and Bob. Once the system enters the laboratory of either experimenter, they toss a fair coin (generate a random bit), and label the result a and b for Alice and Bob respectively. Bob generates a further random bit, labelled b', the result of which determines the objective of the task. After generating these bits, the experimenters may perform operations on the system and then send it out of their laboratory. In all cases, each experimenter then makes a guess of the other's random bit, labelled x and y for Alice and Bob's guess respectively. In the case $b' = 0$, then only Alice's guess is counted. If $b' = 1$ then it is Bob's guess which is counted. If the guess which is counted is correct, then the experimenters have succeeded. The experimenter's probability of success in the task can therefore be written

$$p_{succ} = \frac{1}{2}\Big[p(x = b|b' = 0) + p(y = a|b' = 1)\Big]. \tag{1.19}$$

It is possible to show that, for situations in which there is a definite causal order (DCO), the following bound holds for any strategy [5]:

$$p_{succ}^{DCO} \leq \frac{3}{4}. \tag{1.20}$$

As an example, let us consider the causal order in which Bob receives the system first, and then sends it to Alice. If $b' = 0$ (Alice must guess correctly), then the experimenters will succeed — Bob simply encodes his bit b in the system and then sends it to Alice. However, if $b' = 1$, Bob must guess Alice's bit. This guess will be random however; there is no way for Alice to signal to Bob, since Alice's operations and guesses are in the causal future of those of Bob. Therefore $p(x = b|b' = 0) = 1$, and $p(y = a|b' = 1) = 1/2$, hence the bound is saturated.

In order to treat more general cases, where the causal structure in which the experimenters are embedded is indefinite, we must introduce the process matrix formalism. This formalism will only be touched on here in the interests of brevity, but is treated more thoroughly in other works [5, 9, 10], and will be addressed again in section 4.5. A process matrix maps a set of local operations which are used in an experiment to probability distributions which describe the outcomes of

the experiment. The mapping is determined by the causal relationship between the operations.

To each experimenter we associate an input and an output Hilbert space. In Alice's case these are labelled $\mathcal{H}^{A_1}$ and $\mathcal{H}^{A_2}$, respectively. Within the lab, Alice performs an operation, which has a certain outcome i from the set of all possible outcomes $\{1, ..., n\}$. The transformation from the input to the output state associated with a given outcome i is given by the completely positive (CP) map $\mathcal{M}_i^A : \mathcal{L}(\mathcal{H}^{A_1}) \to \mathcal{L}(\mathcal{H}^{A_2})$, where $\mathcal{L}(\mathcal{H}^X)$ is the space of matrices on the Hilbert space $\mathcal{H}^X$. The sum over all outcomes i of these CP maps is a CPTP map, whose Kraus operators therefore satisfy equation (1.18). The relevant object that we want to compute is the probability distribution of all possible outcomes i for Alice and j for Bob, which are associated with their transformations $\mathcal{M}_i^A$ and $\mathcal{M}_j^B$. This probability distribution we will label with $P(\mathcal{M}_i^A, \mathcal{M}_j^B)$.

It can be shown [5] that the properties of local quantum operations implies that $P(\mathcal{M}_i^A, \mathcal{M}_j^B)$ must be a bilinear function of the maps $\mathcal{M}_i^A$ and $\mathcal{M}_j^B$. This implies that the distribution can be written

$$P(\mathcal{M}_i^A, \mathcal{M}_j^B) = \mathrm{Tr}\Big[W^{A_1A_2B_1B_2}\Big(M_i^{A_1A_2} \otimes M_j^{B_1B_2}\Big)\Big]. \tag{1.21}$$

Where $W^{A_1A_2B_1B_2}$ is the process matrix and $M_i^{A_1A_2}$ and $M_j^{B_1B_2}$ are the Choi-Jamiołkowsky (CJ) [11, 12] matrices of maps $\mathcal{M}_i^A$ and $\mathcal{M}_j^B$ respectively. The requirement that all probabilities $P(\mathcal{M}_i^A, \mathcal{M}_j^B)$ be non-negative for all possible maps implies the condition $W^{A_1A_2B_1B_2} \geq 0$. A further condition on the process matrix is implied by the stipulation that $\sum_{ij} P(\mathcal{M}_i^A, \mathcal{M}_j^B) = 1$, i.e the sum of the probabilities is unity.

As an example of a process matrix for a situation in which there exists a definite causal structure, let us return to the ordering discussed above, where Bob receives an input state ρ^{B_1} and sends his output to Alice via a quantum channel $\mathcal{C}$. This implies that the probabilities are given by

$$P(\mathcal{M}_i^A, \mathcal{M}_j^B) = \mathrm{Tr}\Big[\mathcal{M}_i^A \circ \mathcal{C} \circ \mathcal{M}_j^B(\rho^{B_1})\Big]. \tag{1.22}$$

These probabilities correspond to a process matrix

$$W^{A_1A_2B_1B_2} = \mathbb{I}^{A_2} \otimes C^{B_2A_1} \otimes \rho^{B_1}, \tag{1.23}$$

with $C^{B_2A_1}$ representing the CJ matrix associated with the channel $\mathcal{C}$, which connects Bob's output (B_2) with Alice's input (A_1). This is a process matrix for a situation in which the causal order is definite, and as such, the probabilities, for the communication task described above, $P(\mathcal{M}_i^A, \mathcal{M}_j^B)$ obey the causal inequality of equation (1.20).

The fascinating result derived in [5], is that there are valid process matrices, which obey the laws of local quantum operations, but whose associated causal order is not well defined, for which the causal inequality can be violated. One such example is the matrix

$$W^{A_1A_2B_1B_2} = \frac{1}{4}\Big[\mathbb{I}^{A_1A_2B_1B_2} + \frac{1}{\sqrt{2}}(\sigma_z^{A_2}\sigma_z^{B_1} + \sigma_z^{A_1}\sigma_x^{B_1}\sigma_z^{B_2})\Big], \tag{1.24}$$

where σ_i are the Pauli matrices. This process matrix contains terms which are characteristic to both situations in which Alice is in the causal past of Bob and vice versa. The term $\sigma_z^{A_2}\sigma_z^{B_1}$ allows signalling from Alice to Bob; it represents a connection from Alice's output space (A_2) to Bob's input space (B_1). The term $\sigma_z^{A_1}\sigma_x^{B_1}\sigma_z^{B_2}$ allows signalling from Bob to Alice; it represents a connection from Bob's input and output spaces (B_1 and B_2) to Alice's input space (A_1). Importantly, the full process matrix cannot be broken down into a probabilistic mixture of process matrices which contain only one-way signalling terms of the form $W^{A_1A_2B_1B_2} = qW^{A\prec B} + (1-q)W^{B\prec A}$, where $W^{A\prec B}$ is a process matrix for a situation in which Alice's actions are in the causal past of Bob's and vice versa. It is thus termed non-separable, and is not compatible with any definite or classically random causal structure.

For the process described by equation (1.24), Alice and Bob can violate the causal inequality of equation (1.20) if Bob makes a measurement in a basis which depends on his bit b' which defines their goal. If his bit $b' = 0$, he must communicate his bit b to Alice. He then makes his measurement on the system in the x basis.

Inserting the appropriate CJ operator (which contains the factor $|x_\pm\rangle\langle x_\pm|^{B_1}$) for this measurement into equation (1.21) annihilates the term $\sigma_z^{A_2}\sigma_z^{B_1}$. What remains is a noisy channel from Bob to Alice which can be used to transmit the bit b. If instead $b' = 1$ then Bob must make his measurement on the system in the z basis. Then the term $\sigma_z^{A_1}\sigma_x^{B_1}\sigma_z^{B_2}$ is similarly annihilated, leaving a noisy channel from Alice to Bob, which can be used to transmit the bit a. The resulting success probability from equations (1.19) and (1.21) is

$$p_{succ} = \frac{2+\sqrt{2}}{4} > \frac{3}{4} = \max(p_{succ}^{DCO}). \tag{1.25}$$

The violation of this inequality bears some similarity with that of Bell's inequality [13]. Bell's inequality gives a bound on correlations between measurements on spatially separated systems which obey local realism. This equality can be violated when we relax the requirement of local realism and allow quantum entanglement between the systems. In the case of causal orders, the causal inequality of equation (1.20) holds for all cases in which the causal order of a scenario is definite. As we have seen, in cases where this requirement is relaxed and the causal order is indefinite, this bound can be exceeded, even when the operations embedded in this causal order obey the regular laws of quantum operations. The fact that this violation can be achieved, and that a communication task becomes possible when the causal order is allowed to be indefinite, is a strong motivation to consider further the implications and applications of quantum causal orders, and in what circumstances they might arise.

1.3.2 The Quantum SWITCH

The quantum SWITCH [6] (developed independently from and slightly before [5]) is the main formalism for indefinite causal orders that will be utilised in this thesis. The quantum SWITCH describes the causal structure of a situation, illustrated in figure 1.1, in which the order of application of two operations (e.g $\mathcal{N}_1$ and $\mathcal{N}_2$) is correlated with a control qubit. If the control qubit is in the state $|0\rangle_c$, then operation $\mathcal{N}_1$ is performed first, followed by operation $\mathcal{N}_2$. If the control qubit is

in the state $|1\rangle_c$, then the order is reversed. It is possible for the control qubit to be prepared in a superposition of $|0\rangle_c$ and $|1\rangle_c$ states. In this case, it is not possible to assign a definite causal order to the operations; instead they take place in a superposition of causal orders. For this reason, it is impossible to represent the action of the quantum SWITCH with the two operations placed (once each) in a conventional quantum circuit.

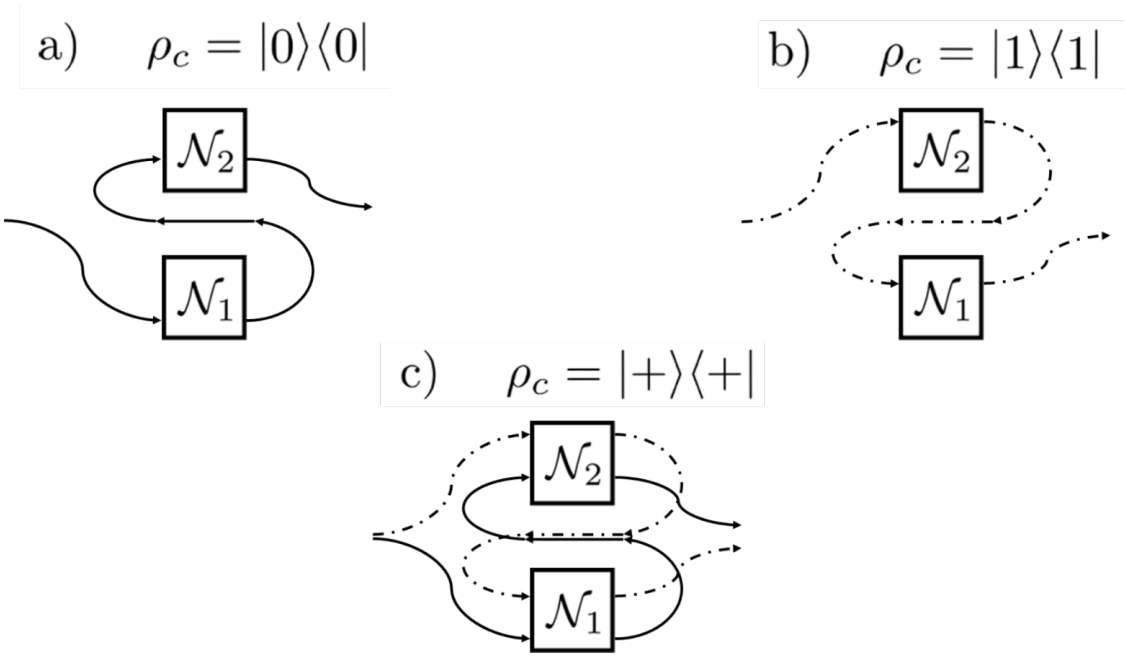


Figure 1.1: (a) and (b) illustrate channels $\mathcal{N}_1$ and $\mathcal{N}_2$ placed in a definite order, corresponding to the control qubit being in state $|0\rangle\langle 0|$ and $|1\rangle\langle 1|$ respectively. In (c) the quantum SWITCH places the channels in a superposition of causal orders. It entangles the order of the two channels with the state of the control qubit, in this case $|+\rangle\langle +|$.

Mathematically, the quantum SWITCH is a superoperator: it maps quantum channels to quantum channels. The output channel $\mathcal{S}$ of the quantum SWITCH, with input channels $\mathcal{N}_1$ and $\mathcal{N}_2$, acts on the product of a control and a target subspace $\mathcal{H}^c \otimes \mathcal{H}^T$, and takes the form, analogously with equation (1.16),

$$\mathcal{S}(\mathcal{N}_1, \mathcal{N}_2)(\rho_c \otimes \rho) = \sum_{i,j} W_{ij}(\rho_c \otimes \rho)W_{ij}^\dagger. \tag{1.26}$$

Here W_{ij} are the Kraus operators of the new channel, and ρ_c and ρ are the initial states of the control qubit and the target system respectively. The Kraus operators themselves take the form

$$W_{ij} = |0\rangle\langle 0|_c \otimes K_i^{(2)} K_j^{(1)} + |1\rangle\langle 1|_c \otimes K_j^{(1)} K_i^{(2)}, \tag{1.27}$$

where $K_j^{(1)}$ and $K_i^{(2)}$ are the Kraus operators of channels $\mathcal{N}_1$ and $\mathcal{N}_2$ respectively, and act on the target system. These Kraus operators satisfy the completeness relation of equation (1.18), $\sum_{ij} W_{ij}^\dagger W_{ij} = \mathbb{I}$, assuming that the Kraus operators of the constituent channels also satisfy the completeness relation. This ensures that the new channel is a valid quantum channel. Despite this fact, it has been shown [6] that it is not possible to generate the output of the quantum SWITCH in the quantum circuit picture without using more than a single instance of $\mathcal{N}_1$ or $\mathcal{N}_2$, or including a closed time-like curve. In some contexts, this might represent a problematic increase in the resources necessary to complete a task.

In fact, it is possible to use the process matrix formalism described above to represent the causal structure of the quantum SWITCH precisely. To understand the quantum SWITCH in the process matrix framework as described above, we may simply consider the channels $\mathcal{N}_1$ and $\mathcal{N}_2$ to represent the actions of two experimenters contained within two closed laboratories. This has been done in [14], where it was shown that the quantum SWITCH can be represented by a process involving four parties (or experimenters as termed above). The associated process matrix is non-separable, confirming that the operation of the quantum SWITCH is indeed incompatible with a fixed causal order between the operations.

1.3.3 Physical Realisation

If and how a quantum SWITCH, or an indefinite causal order more generally, can be physically realised is the subject of ongoing discussion. This debate centres around whether tabletop experiments have been able to faithfully realise the quantum SWITCH. One of the original motivations for considering such causal structures is the possibility that they might be a feature of a quantum theory of gravity [4]. In general relativity, the causal relations between events are determined by the metric, which is itself determined by the positions of massive objects. Since, in quantum theory, massive objects can be in superpositions of positions, it is then

natural to consider the possibility that these superposed masses might give rise to superpositions of causal orders. A simple example has been hypothesised [15], which involves the superposition of one massive object (e.g. a planet!), with each branch of the superposition inducing a different causal order of events.

More conventional experiments, however, have been performed, which are claimed to exhibit indefinite causal orders in the form of the quantum SWITCH. The majority of these are tabletop photonic experiments [16–22]. Recently there has been a nuclear magnetic resonance (NMR) approach put forward [23]. There has been some debate over whether such experiments really do constitute faithful implementations of the quantum SWITCH. With some, for example Ref. [24], arguing that in such implementations it is not correct to say that each channel only operates once. On the other hand, some [10] have argued, using the process matrix formalism, that these implementations are faithful, since they have the correct process matrix. We will leave further discussion of this point for chapter 4, where we will discuss this question more, in light of the results presented therein.

1.3.4 Applications

The use of indefinite causal orders to violate the bound of equation (1.20) for the success probability of a particular communication task indicates that indefinite causal orders might enable other, more useful tasks to be performed. This has turned out to be the case. In particular, the quantum SWITCH has been shown to provide advantages in quantum computation [25–27], communication [28–30], and metrology [31–33].

In the field of quantum computation, ICOs have been shown to reduce from two to one the number of queries required to discriminate between channels with commuting and anti-commuting Kraus operators [25]. The quantum SWITCH has been shown [26] to allow the programming of all permutations of a series of N unitary channels with just one use of each channel, where a conventional quantum circuit would require N uses of each channel. The quantum SWITCH has been used

[27] to reduce the number of queries required to determine the unique property from a list of $n!$ properties that a list of n matrices all satisfy from $\mathcal{O}(n^2)$ to $\mathcal{O}(n)$ queries.

In quantum metrology, a protocol [33] using the quantum SWITCH has been developed which outperforms any definite causal ordered protocol for a task which involves estimating the average displacements that a series of black boxes impart to a harmonic oscillator. There are $2N$ boxes, half of which impart a position displacement and the other half a momentum displacement. These displacements are independent from each other. The task is to estimate the product of the average displacements in position and momentum, and the root mean square error (RMSE) scales as $1/N$ for the optimal fixed causal order protocol. The quantum SWITCH protocol however, achieves an RMSE which scales as $1/N^2$. Other quantum SWITCH protocols have shown an increase in Fisher information obtained when compared to definite causal order protocols for thermometry [31] and channel identification [32].

Communication channels which have zero information capacity can become useful when combined using a quantum SWITCH [30]. One particular protocol [28] is of particular interest, since the completely depolarising channel, which is 'activated' by the quantum SWITCH, is the quantum communication analogue of the thermalising channel in quantum thermodynamics, which will be studied in the following chapter.

This is a haiku
Haikus don't have to make sense
Refrigerator

—Anonymous

2

Quantum Refrigeration with Indefinite Causal Order

Contents

2.1 Thermalising Channels in an Indefinite Causal Order— 19
2.2 Simulation Quantum Circuit 22
2.3 ICO Refrigerator 23
2.3.1 Two-level Refrigeration Cycle 24
2.3.2 Three-level Refrigeration Cycle 27
2.4 Performance of the Refrigerators 28
2.4.1 Two-level Refrigerator Performance 28
2.4.2 Three-level Refrigerator Performance 32
2.5 Discussion 34

This chapter is based on a paper which was published in *Physical Review Letters* in August 2020 [34]. The author of this thesis was responsible for all the main results of this project.

2.1 Thermalising Channels in an Indefinite Causal Order—

Recent work [28, 29] has demonstrated the counter-intuitive result that two completely depolarising channels, when placed in an indefinite causal order, can transmit information. This is despite the fact that these channels have no information capacity

when used in any fixed or classically random ordering. The action of the fully depolarising channel $\mathcal{N}^D$ can be represented by uniform randomisation over d^2 orthogonal unitary operators U_i

$$\mathcal{N}^D(\rho) = \mathrm{Tr}[\rho]\frac{I}{d} = \frac{1}{d^2}\sum_i^{d^2} U_i \rho U_i^\dagger. \tag{2.1}$$

Recalling equation (1.16), the Kraus operators for this channel are $K_i^D = \frac{1}{d}U_i$. It is evident that this channel is constant, and as a result it has no information capacity. However, when two of these channels are used in an indefinite causal order, non-zero Holevo information can be transmitted. We would like to exploit the intimate relationship between information theory and thermodynamics, so we turn to thermalising channels - the closest equivalent to depolarising channels in the world of thermodynamics. A completely thermalising channel is defined by a certain inverse temperature β, and maps any input state ρ to the output state τ, which is a thermal state with effective inverse temperature β. The density operator representing the state τ in the energy basis is a diagonal matrix with entries $\frac{1}{Z}e^{-\beta E_j}$, where E_j are the energy eigenvalues of the system's Hamiltonian and Z is the normalising partition function. The action of the thermalising channel $\mathcal{N}^\tau$ is

$$\mathcal{N}^\tau(\rho) = \mathrm{Tr}[\rho]\tau = \frac{1}{d}A\left(\sum_i^{d^2} U_i \rho U_i^\dagger\right)A^\dagger, \tag{2.2}$$

where A is the square root of the diagonal matrix τ. It can be easily seen, in the second equality of equations (2.1) and (2.2), that from the depolarising channel to the thermalising channel the Kraus operators change from

$$K_i^D = \frac{1}{d}U_i \longrightarrow K_i^\tau = \sqrt{\frac{1}{d}}AU_i. \tag{2.3}$$

The new operators do indeed satisfy the requirement for Kraus operators that $\sum_i K_i^{\tau\dagger}K_i^\tau = I$, since the set $\{U_i^\dagger\}$ is also a set of orthogonal unitary operators, and so equation (2.1) can be used to obtain identity.

We now calculate the result when two identical thermalising channels in an indefinite causal order are applied to a state ρ and control system ρ_c. If the control

system is initialised in the state $\rho_c = |\psi_c\rangle\langle\psi_c|$, where $|\psi_c\rangle = \sqrt{\alpha}\,|0\rangle + \sqrt{1-\alpha}\,|1\rangle$, then the output state, after interaction with the thermalising channels in an indefinite causal order, will be:

$$\begin{aligned}
S(\mathcal{N}^\tau,\mathcal{N}^\tau)(\rho_c\otimes\rho) = \frac{1}{d^2}\sum_{i,j}\Big(&\alpha\,|0\rangle\langle 0|_c \otimes AU_iAU_j\rho U_j^\dagger A^\dagger U_i^\dagger A^\dagger \\
&+(1-\alpha)\,|1\rangle\langle 1|_c \otimes AU_jAU_i\rho U_i^\dagger A^\dagger U_j^\dagger A^\dagger \\
&+\sqrt{\alpha(1-\alpha)}\,|0\rangle\langle 1|_c \otimes AU_iAU_j\rho U_i^\dagger A^\dagger U_j^\dagger A^\dagger \\
&+\sqrt{\alpha(1-\alpha)}\,|1\rangle\langle 0|_c \otimes AU_jAU_i\rho U_j^\dagger A^\dagger U_i^\dagger A^\dagger\Big) \\
= \sum_i \frac{\alpha}{d}\,|0\rangle\langle 0|_c \otimes AU_i\tau U_i^\dagger A^\dagger + \sum_j \frac{1-\alpha}{d}\,|1\rangle\langle 1|_c \otimes AU_j\tau U_j^\dagger A^\dagger \\
+\frac{\sqrt{\alpha(1-\alpha)}}{d}\sum_j\Big(|0\rangle\langle 1|_c \otimes \tau\mathrm{Tr}[U_j\rho A]U_j^\dagger A^\dagger + |1\rangle\langle 0|_c \otimes A\mathrm{Tr}[A^\dagger\rho U_j^\dagger]U_j\tau\Big) \\
= (\alpha\,|0\rangle\langle 0|_c + (1-\alpha)\,|1\rangle\langle 1|_c)\otimes\tau + \sqrt{\alpha(1-\alpha)}\,(|0\rangle\langle 1|_c + |1\rangle\langle 0|_c)\otimes\tau\rho\tau. \quad (2.4)
\end{aligned}$$

The first equality is given by the application of the quantum SWITCH in equation (1.26). The second equality is the action of the depolarising channel in equation (2.1). In the third equality, the diagonal terms are computed by another application of the depolarising channel, and the off diagonal terms are computed using the fact that the operators U_j form an orthonormal basis for the set of $d \times d$ matrices.

Instead of thermalising to the expected thermal state τ, the final state of the system is, in general, different. We note that the final state of the system is entangled with the state of the control qubit. If the control qubit is measured in the computational basis, then the system will be found in the thermal state τ. However, if the control qubit is measured in the $\{|+\rangle_c, |-\rangle_c\}$ basis then we recover:

$$_c\langle\pm|\,S(\mathcal{N}^\tau,\mathcal{N}^\tau)(\rho_c\otimes\rho)\,|\pm\rangle_c = \frac{1}{p_\pm}\Big[\frac{\tau}{2} \pm \sqrt{\alpha(1-\alpha)}\tau\rho\tau\Big], \quad (2.5)$$

with,

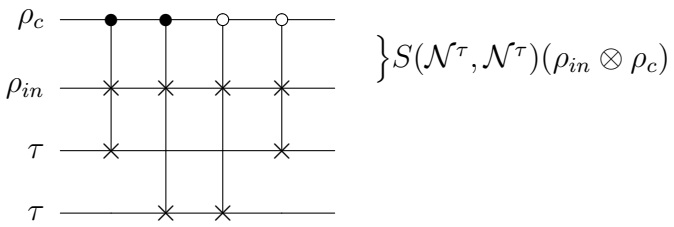
$$p_\pm = \mathrm{Tr}\Big[\frac{\tau}{2} \pm \sqrt{\alpha(1-\alpha)}\tau\rho\tau\Big], \quad (2.6)$$

giving the probabilities of measuring the control qubit in the states $|+\rangle_c$ or $|-\rangle_c$.

Two features of this result should be noted. First, the final state preserves some dependence on the initial state ρ. This is counter-intuitive, since ordinarily the thermalising channels would remove any such dependence. Secondly, the effective temperature of the final state will be different than that of the expected thermal state τ. The reason for this result is that the Kraus operators of the thermalising channels do not commute with one another, so the action of the quantum SWITCH of the two identical channels is non-trivial. The temperature of the final state will be higher or lower, depending on whether the $|+\rangle_c$ or $|-\rangle_c$ state is measured on the control qubit. It is this fact that we will exploit to perform refrigeration.

2.2 Simulation Quantum Circuit

It is possible to construct a unitary quantum circuit which acts on the system plus environments and has the same output as the quantum SWITCH of the thermalising channels.



Here, the order in which the swaps occur is determined by the state of the control qubit. The label after the upper two wires indicates that the marginal state on the control and working qubits at the output of this circuit is identical to $S(\mathcal{N}^\tau,\mathcal{N}^\tau)(\rho\otimes\rho_c)$ in equation (2.4). Although there are, in principle, an infinite number of circuits with different environments which give this output, this particular representation is helpful for thermodynamic considerations, because the environments (two bottom inputs τ) can be thought of as qubits randomly drawn from a reservoir which is a thermal bath of qubits each with thermal state τ. For any energy-conserving unitary circuit which commutes with the overall Hamiltonian of the qubits, the free energy of

the output is equal to the free energy of the inputs. The only subsystem of the input state that has non-zero free energy in the case when $\rho_{in} = \tau$, is the control, since all the other inputs are in a thermal state. In this case, which we discuss below, some of the free energy in the control is then distributed to the system and the reservoir environments. Although the output of the circuit is the same as that of the quantum SWITCH of two thermalising channels, the circuit uses controlled thermalising channels, and two of each such channels, and so is not operationally equivalent, in that the requirements for its execution are different. The circuit is provided here to aid intuition about what is happening, thermodynamically speaking, during the quantum SWITCH of two thermalising channels. It will be returned to in chapter 3.

2.3 ICO Refrigerator

A natural question is whether the ability to perform operations in an ICO can be useful in performing thermodynamic tasks. The fact that a system can 'thermalise' with identical reservoirs, while the resulting state has a temperature not equal to the temperature of the reservoirs, suggests that this is the case.

For simplicity, we will consider the situation where the working system has two energy eigenstates - a ground and an excited state, $|g\rangle$ and $|e\rangle$. This assumption simplifies our considerations, because in a two-level system every state can be assigned a consistent effective temperature. The Hamiltonian for the system is defined as $H = \Delta |e\rangle \langle e|$. Since we are interested in these operations in the context of thermodynamic work cycles, let us restrict ourselves to thermal initial states. Then the density matrix for the initial state is

$$\rho = \frac{1}{Z_\rho} \begin{pmatrix} 1 & 0 \\ 0 & e^{-\beta_\rho \Delta} \end{pmatrix}, \quad Z_\rho = 1 + e^{-\beta_\rho \Delta}, \tag{2.7}$$

where β_ρ is the state's inverse temperature. We also note that the state obtained after thermalising classically with the reservoir is

$$\tau = \frac{1}{Z_\tau} \begin{pmatrix} 1 & 0 \\ 0 & e^{-\beta_\tau \Delta} \end{pmatrix}, \quad Z_\tau = 1 + e^{-\beta_\tau \Delta}. \tag{2.8}$$

Let us take our initial state and the reservoirs to be at the same temperature, *i.e* $\beta_\rho = \beta_\tau = \beta$, and $Z_\rho = Z_\tau = Z$. Using equation (2.5), and setting $\alpha = \frac{1}{2}$ (an equal superposition of orders), the resulting state after ICO thermalisation and control system measurement is:

$$\rho_{ICO} = \frac{\rho'_{ICO}}{\mathrm{Tr}[\rho'_{ICO}]}, \quad \rho'_{ICO} = \begin{pmatrix} 1 \pm \frac{1}{Z^2} & 0 \\ 0 & e^{-\beta\Delta} \pm \frac{e^{-3\beta\Delta}}{Z^2} \end{pmatrix}. \tag{2.9}$$

After this transformation, the system is at a different temperature than the reservoir. Hence one can create a thermodynamic cycle, the operation of which transfers heat from colder to hotter reservoirs, while consuming purity in the control qubit, or, equivalently, consuming work due to the erasure of the results of measurement.

We will consider two related protocols, which differ in the number of reservoirs and associated temperature levels that the refrigerator runs between. In this section, the steps of the refrigeration cycles will be outlined. A detailed mathematical description of the changes which accompany each step and the overall performance of the cycle can be found in section 2.4.

2.3.1 Two-level Refrigeration Cycle

For the first protocol, the two-level refrigerator, there are two relevant temperatures, β_C and β_H, for the hot and cold reservoirs respectively. Since the quantum SWITCH requires two channels, the cold reservoir is divided into at least two sub-reservoirs. The working system starts at the temperature of the cold reservoirs.

The cycle is illustrate in figure 2.1. In the first step (i), two of the cold reservoirs are placed in an indefinite causal order using the quantum SWITCH, and the working system 'thermalises' with them. The control qubit is measured in the $\{|+\rangle_c, |-\rangle_c\}$ basis and the result is placed in a memory. In the second step (ii), if the result of the measurement in step (i) was $|-\rangle_c$, then the system has heated up and is thermalised classically with the hot reservoir. In the case that $|+\rangle_c$ was measured, this step is skipped (no operation is performed). In the third step (iii),

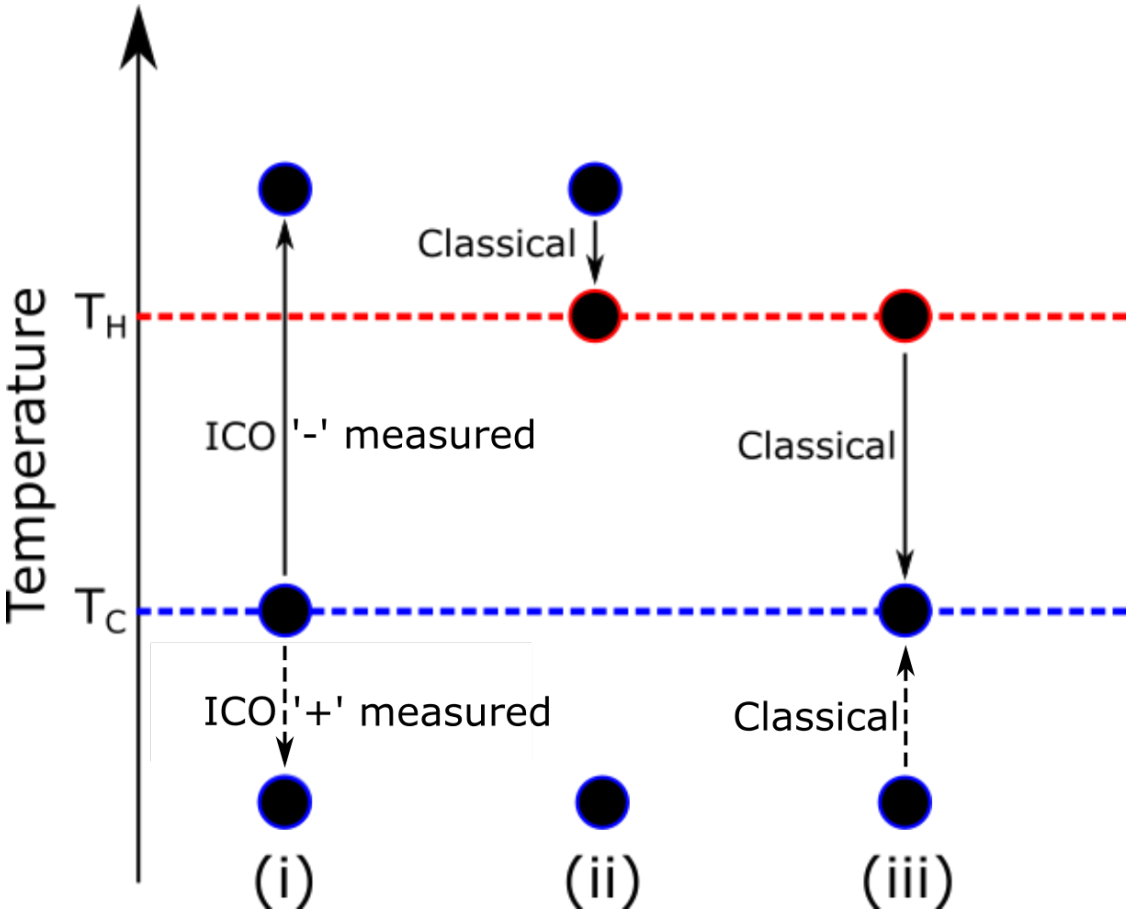


Figure 2.1: The three steps of the refrigeration cycle of the two-level ICO Fridge. The black dot represents the working system, and the colour of the outline indicates the temperature of the last reservoir(s) with which it has interacted. In step (i) the working system undergoes thermalisation in an ICO with the cold reservoirs. The solid lines represent the operations in the event of a measurement of $|-\rangle_c$ for the state of the control system in step (i), whereas the dotted lines represent those in the event of a measurement of $|+\rangle_c$. In step (ii), if the result of the measurement was $|-\rangle_c$, the working system is thermalised classically with the hot reservoir. In step (iii) the working system is thermalised classically with the cold reservoir to complete the cycle.

the system is thermalised classically with a cold reservoir, and all the cold reservoirs are thermalised classically with one another, so that they remain identical.

In step (i), averaging over both possible measurement results, there is no net transfer of heat, either from the reservoirs to the working system or from these systems to an outside system. This statement is justified in the calculations of the fridge's performance in section 2.4. In step (ii), the net result is that heat is transferred from the working system to the hot reservoir. In step (iii), therefore, the net result must be that heat is transferred from the reservoirs to the working

system. Since this is the only step which involves a net heat change for the cold reservoirs, it can be deduced that the overall action of the cycle is to transfer heat from the cold to the hot reservoirs.

The conclusion that heat is transferred from the cold to hot reservoirs can also be drawn by considering heat transfers from the set of systems comprised of the cold reservoirs, the working system, and the control qubit. The only step of the protocol in which these systems interact with a system outside this set is step (ii), whose net outcome is a heat transfer to the hot reservoir and, therefore, out of the set. However, the working system is returned to its initial state in step (iii), and the control qubit has zero heat capacity. The only system in the set, therefore, which could have undergone a heat flow is the cold reservoir. Hence, it can be concluded that the overall result of the cycle is that heat flows from the cold to the hot reservoirs.

It is important to note that despite the fact that a measurement is made in the process of the operation of the refrigeration cycle, and the next step is conditioned on the result of this measurement, the cycle does not rely on post-selection to gain its advantage. The outcomes where an undesired result is measured are fully accounted for in the consideration of the average thermodynamic performance of the cycle.

In fact, there is an equivalent cycle without a projective measurement at all. Instead of measuring the control qubit at the end of step (i), the execution of step (ii) is controlled (on the state $|-\rangle_c$) by the control qubit, and step (iii) is carried out as normal. The end result will be a superposition of a branch where the control qubit is in the state $|+\rangle_c$, and a branch where the control qubit is in the state $|-\rangle_c$. The average heat flow over the two branches will be from the cold to the hot reservoirs. To run the cycle again, the old control qubit is discarded and a new control qubit in the state $|+\rangle_c$ must be introduced. Once the old control qubit is discarded, the remaining systems must be represented by a mixed state, making the situation identical to that described above. When implemented in this way, the cycle consumes free energy from the purity in the control qubit, rather than the work cost of measurement, to run. The two implementations are thermodynamically equivalent.

2.3.2 Three-level Refrigeration Cycle

The three-level refrigeration cycle makes use of an ensemble of 'middle' reservoirs, with a temperature β_M between that of the hot and cold reservoirs. The working system starts at the temperature of the middle reservoirs.

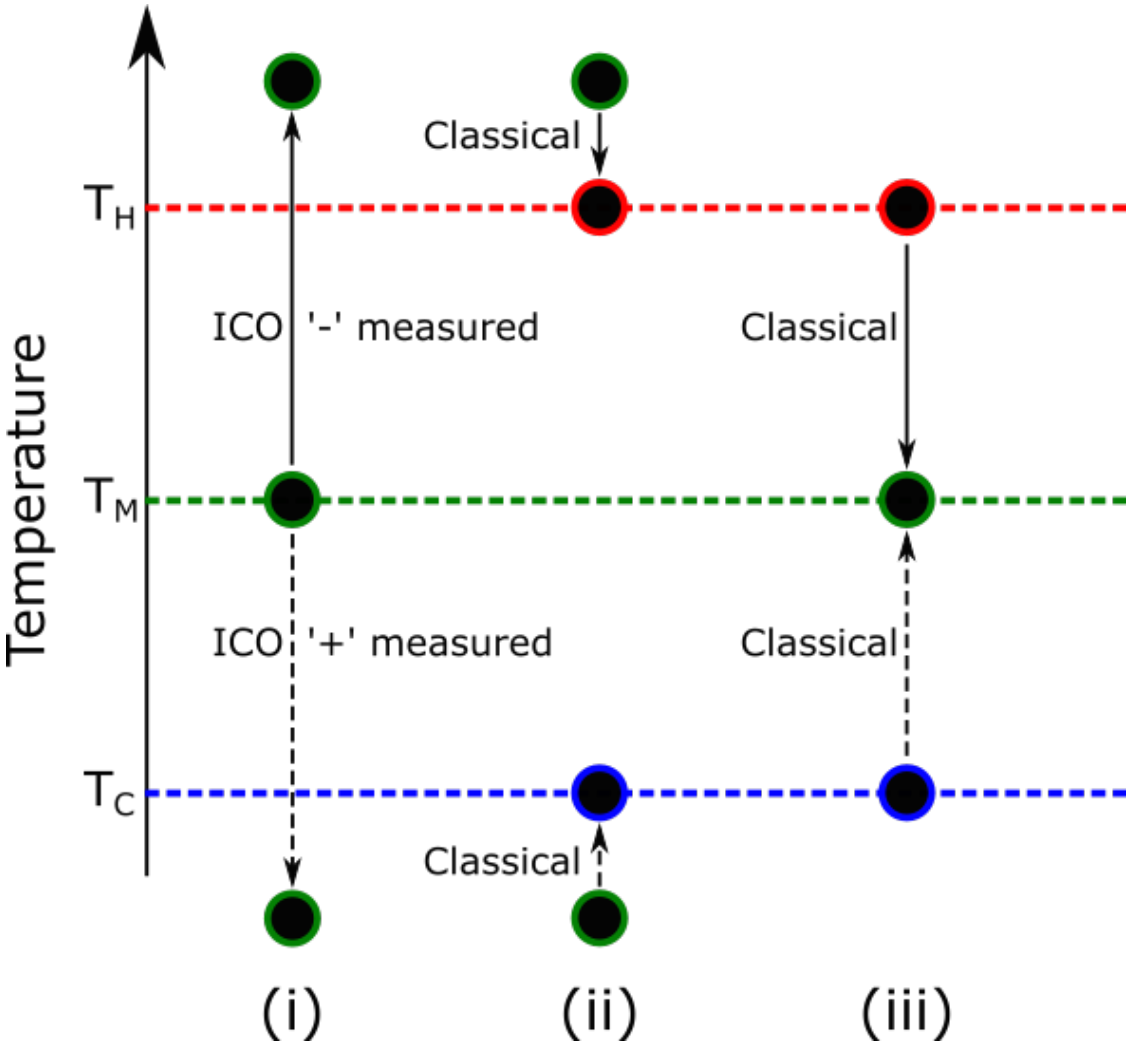


Figure 2.2: The three steps of the refrigeration cycle of the three level ICO Fridge. The solid lines again represent the operations in the event of a measurement of $|-\rangle_c$ for the state of the control system in step (i), and the dotted lines represent those in the event of a measurement of $|+\rangle_c$. The cycle is similar to that of the two-level fridge, except for the addition of the colder reservoir and the fact that a thermalisation is performed in step (ii) regardless of the measurement result in step (i).

In the first step (i), two of the middle reservoirs are placed in an indefinite causal order using the quantum SWITCH, and the working system 'thermalises' with them. The control qubit is measured. If the control qubit is found in the state

$|-\rangle_c$, the working system will now be at a higher temperature. If it is measured in the state $|+\rangle_c$, then it will now be at a lower temperature.

The action taken in the second step (ii) depends on the result of the control qubit measurement in step (i). If $|-\rangle_c$ was measured, then the working system is thermalised classically with the hot reservoir. If $|+\rangle_c$ was measured, then the working system is thermalised classically with the cold reservoir. In the third step (iii), the working system is thermalised classically with a middle reservoir, and all the middle reservoirs are thermalised classically with one another, so that they remain identical.

Let us consider the heat changes that accompany each step. In step (i) only the middle reservoirs are involved. Conservation of energy, and calculations performed in section 2.4 imply that when both measurement results are taken into account, there is no net heat flow from the reservoirs. In step (ii), in the case that $|-\rangle_c$ was measured, heat is transferred from the working system to the hot reservoir. In the opposite case, heat flows out of the cold reservoir into the working system. In step (iii), for the $|-\rangle_c$ case, heat is transferred from the working system to the middle reservoirs, for the $|+\rangle_c$ case, the flow of heat is reversed. We will see that it is possible to configure the temperatures of the reservoirs so that the net result of step (iii) is zero heat flow. In this case, then the only relevant heat flows for determining the net result of the cycle are those of step (ii), and it can be deduced that the overall action of the cycle is to transfer heat from the cold to the hot reservoirs.

2.4 Performance of the Refrigerators

2.4.1 Two-level Refrigerator Performance

In this subsection the performance characteristics of the two-level quantum fridge are derived. The average heat flow per cycle is calculated, then the work cost per cycle and hence the efficiency of the fridge are determined. The performance of the ICO fridge is dependent on the temperatures of the hot and cold reservoirs and the Hamiltonian of the working substance. In order to calculate heat flows, we assume that all thermalisations are isochoric, *i.e.* that all changes in internal energy correspond to heat flows to or from the relevant systems.

First, let us examine the net heat changes accompanying the first step of the cycle, justifying comments made in the previous section. The net heat flow to the working system during this step is given by

$$\delta Q_W^{(\mathrm{i})} = p_+ \delta Q_W^{+(\mathrm{i})} + p_- \delta Q_W^{-(\mathrm{i})}, \tag{2.10}$$

where $p_\pm$ are the probabilities of the two possible measurements of the control qubit, and $\delta Q_W^{\pm(\mathrm{i})}$ are the heat changes accompanying step (i) when $\pm$ is measured, themselves given by

$$\delta Q_W^{\pm(\mathrm{i})} = \mathrm{Tr}[\rho_W^{\pm(\mathrm{i})} H] - \mathrm{Tr}[\rho_W^{(0)} H], \tag{2.11}$$

where $\rho_W^{(0)}$ and H are the initial state and the Hamiltonian of the working system respectively.

Equation (2.5) gives the state of the working system after ICO thermalisation and measurement:

$$\rho_W^{\pm(\mathrm{i})} = \frac{\tau \pm \tau\rho_W^{(0)}\tau}{\mathrm{Tr}[\tau \pm \tau\rho_W^{(0)}\tau]} = \frac{\tau \pm \tau\rho_W^{(0)}\tau}{p_\pm}. \tag{2.12}$$

Combining these expressions we obtain the net heat change

$$\begin{aligned}\delta Q_W^{(\mathrm{i})} &= \mathrm{Tr}[(\tau + \tau\rho_W^{(0)}\tau)H] - \mathrm{Tr}[(\tau + \tau\rho_W^{(0)}\tau)H]\mathrm{Tr}[\rho_W^{(0)} H] \\ &\quad + \mathrm{Tr}[(\tau - \tau\rho_W^{(0)}\tau)H] - \mathrm{Tr}[(\tau - \tau\rho_W^{(0)}\tau)H]\mathrm{Tr}[\rho_W^{(0)} H] \\ &= 2\mathrm{Tr}[(\tau - \rho_W^{(0)})H] = 0.\end{aligned} \tag{2.13}$$

The last equality comes from the initial conditions of the cycle — the working system starts in a thermal state at the same temperature as the reservoirs ($\rho_W^{(0)} = \tau$). Since there is no flow of heat from the working system, we conclude that there is likewise no flow of heat from the reservoirs. There is no other system to which this heat could flow; the control qubit is the only other system involved in this step, and it has zero heat capacity. Equivalently, straightforward energy conservation implies the same conclusion.

Now the net heat change per cycle is calculated. As in section 2.3, let us consider the heat flows from the set of systems which is comprised of the cold reservoirs,

working system, and control qubit. The only step in which any member of this set interacts with a system outside this set is step (ii). The net heat flow into the working system during this step is given by

$$\delta Q_W^{(\mathrm{ii})} = p_- \mathrm{Tr}[(\rho^{-(\mathrm{ii})} - \rho^{-(\mathrm{i})})H]. \tag{2.14}$$

Here $\rho^{-(\mathrm{ii})}$ and $\rho^{-(\mathrm{i})}$ denote the state of the working system after steps (ii) and (i) respectively. The subscript W has been suppressed to reduce the density of notation. Only the branch of the cycle in which $|-\rangle_c$ is measured is considered, since in the other branch no operation is performed during step (ii).

Writing the initial state of the working system

$$\rho^{(0)} = \frac{1}{Z_C}\begin{pmatrix} 1 & 0 \\ 0 & r_C \end{pmatrix}, \quad Z_C = 1 + r_C, \tag{2.15}$$

where we have taken $r_x = e^{\beta_x \Delta}$ to ease the burden of notation, equation (2.9) gives the unnormalised state of the working system after step (i) with a measurement of $|-\rangle_c$ on the control qubit as

$$\rho^{-(\mathrm{i})} = \begin{pmatrix} \frac{1}{Z_C} & 0 \\ 0 & \frac{r_C}{Z_C} \end{pmatrix} - \begin{pmatrix} \frac{1}{Z_C^3} & 0 \\ 0 & \frac{r_C^3}{Z_C^3} \end{pmatrix}. \tag{2.16}$$

This expression can be manipulated to yield the normalised state

$$\rho^{-(\mathrm{i})} = \frac{r_C + 2}{3r_C + 3}\begin{pmatrix} 1 & 0 \\ 0 & \frac{2r_C + 1}{r_C + 2} \end{pmatrix}. \tag{2.17}$$

The state of the working system after thermalising with the hot reservoir in step (ii) is

$$\rho^{-(\mathrm{ii})} = \frac{1}{1 + r_H}\begin{pmatrix} 1 & 0 \\ 0 & r_H \end{pmatrix}, \tag{2.18}$$

and equation (2.14) therefore implies the net heat transfer to the working system during this step is

$$\delta Q_W^{(\mathrm{ii})} = p_-[\rho_{(2,2)}^{-(\mathrm{ii})} - \rho_{(2,2)}^{-(\mathrm{i})}]\Delta = p_-\Big[\frac{r_H}{1 + r_H} - \frac{2r_C + 1}{3(1 + r_C)}\Big]\Delta. \tag{2.19}$$

Here the index $(2,2)$ labels the relevant element of a density matrix. This heat flow represents the only flow from our set of systems. Since in step (iii) the working system is returned to its initial state and the control qubit has zero heat capacity, we therefore conclude that the net heat flow to the cold reservoirs over the full cycle is

$$\delta Q_{Cold}^{cycle} = \delta Q_W^{(\mathrm{ii})} = p_- \Big[\frac{e^{-\beta_H \Delta}}{1+e^{-\beta_H \Delta}} - \frac{2e^{-\beta_C \Delta}+1}{3(1+e^{-\beta_C \Delta})} \Big] \Delta, \tag{2.20}$$

where we have replaced the shorthand notation. This relation implies that there is a range of temperatures over which the fridge can operate successfully, defined by the 'positive refrigeration' condition

$$\frac{2e^{-\beta_C \Delta}+1}{3\left(e^{-\beta_C \Delta}+1\right)} > \frac{e^{-\beta_H \Delta}}{1+e^{-\beta_H \Delta}}. \tag{2.21}$$

This condition is equivalent to ensuring that after step (i) of the cycle, the effective temperature of the working substance is higher than the temperature of the hot reservoir.

The work cost associated with the running of the cycle arises from the measurement performed in step (i). Each time a measurement is made, the result of the measurement must be stored in a register. The cycle then proceeds according to the value in the register. Once the result of the measurement is no longer needed then the register must be erased in order to return it to its initial state. Since the measurement itself can be performed with no energy cost (since the control qubit is assumed to have a zero Hamiltonian), the energy cost comes from this process of erasure [35], otherwise known as Landauer's erasure [36].

In the case of a projective measurement, with operators $\{P_k\}$, on a system ρ, the probability of a given outcome is given by $p_k = \mathrm{Tr}[P_k \rho]$. After the measurement the Shannon entropy of the register ρ_M is given by

$$S(\rho_M) = -\sum_k p_k \ln(p_k). \tag{2.22}$$

The energy cost to reset the register in contact with a resetting reservoir with inverse temperature β_R is then

$$\delta W_E = \frac{1}{\beta_R} S(\rho_M). \tag{2.23}$$

In the case of the measurement in step (i) of our cycle, the probabilities for measurement are given by equation (2.6)

$$p_\pm = \mathrm{Tr}\Big[\frac{\tau}{2} \pm \sqrt{\alpha(1-\alpha)}\tau\rho\tau\Big], \tag{2.24}$$

and so the work cost for erasure is

$$\delta W_E = \frac{1}{\beta_R} \sum_\pm p_\pm \ln(p_\pm). \tag{2.25}$$

The coefficient of performance can then be calculated by dividing the heat transfer from the cold reservoir in equation (2.20) by this work cost:

$$\eta_{COP} = -\frac{Q^{cycle}_{Cold}}{\delta W^{cycle}} = \frac{p_- \beta_H}{\sum_\pm p_\pm \ln(p_\pm)} \Big[\frac{e^{-\beta_H \Delta}}{1+e^{-\beta_H \Delta}} - \frac{2e^{-\beta_C \Delta}+1}{3(1+e^{-\beta_C \Delta})}\Big]\Delta, \tag{2.26}$$

where we have chosen the hot reservoir as the resetting reservoir ($\beta_R = \beta_H$).

The efficiency of the fridge is on the order of the Carnot efficiency for a very low temperature cold reservoir and a suitably chosen hot reservoir, but for most parameters the efficiency is much lower. The reason for the cycle's reduced efficiency is that during step (i) there are correlations produced in the reservoirs which are not utilised, but simply allowed to 'thermalise away'. In addition, the thermalising procedures in steps (ii) and (iii) are irreversible isochoric thermalisations. It is likely that a related scheme, which instead used reversible processes, would achieve an efficiency closer to the Carnot bound for more general parameters.

2.4.2 Three-level Refrigerator Performance

The properties of the three-level refrigeration cycle are very similar to those of the two-level cycle. There are three relevant temperatures, that of the cold reservoir β_C, the middle reservoirs β_M and the hot reservoir β_H. The aim of the cycle is to transfer heat from the cold to the hot reservoir. As such, the middle reservoirs should be

considered as part of the machinery of the cycle, and so must, on average, be left unchanged by the cycle as a whole. It was shown in the preceding subsection (2.4.1) that during the ICO step there is no heat flow from the participating reservoirs (in this case the middle reservoirs). Since the middle reservoirs do not participate in step (ii) of the cycle, their net heat change in step (iii) must be zero, so that they remain undisturbed by the cycle:

$$\delta Q_M^{(iii)} = -\delta Q_W^{(iii)} = -(p_+ \delta Q_W^{+(iii)} + p_- \delta Q_W^{-(iii)}) = 0. \tag{2.27}$$

Since $\delta Q_W^{\pm(iii)}$ is determined by the temperatures of the three reservoirs, this relation gives a constraint which fixes the temperature of the middle reservoirs β_M for a given β_C and β_H.

The net heat change per cycle for the cold reservoir is $p_+ \delta Q_C^{+(ii)}$, since this reservoir is only involved in the cycle in step (ii), and only if $|+\rangle_c$ is measured on the control qubit. This heat change can be derived in terms of $p_- \delta Q_W^{-(ii)}$, which has already been calculated above. This is because, since the working system returns to its initial state, we must have

$$\delta Q_W^{cycle} = \delta Q_W^{(i)} + \delta Q_W^{(ii)} + \delta Q_W^{(iii)} = 0. \tag{2.28}$$

The first term of this sum has been shown to be zero in equation (2.13). The third term must be set to zero as in equation (2.27), by choosing the correct temperature β_M for the middle reservoirs. This leaves

$$\delta Q_W^{(ii)} = p_+ \delta Q_W^{+(ii)} + p_- \delta Q_W^{-(ii)} = 0 \implies p_+ \delta Q_C^{+(ii)} = p_- \delta Q_W^{-(ii)}, \tag{2.29}$$

since the heat which flows into the working system in the $|+\rangle_c$ branch of step (ii) flows directly from the cold reservoir ($p_+ \delta Q_W^{+(ii)} = -p_+ \delta Q_C^{+(ii)}$). Utilising equation (2.20), we therefore write

$$\delta Q_C^{cycle} = p_+ \delta Q_C^{+(ii)} = p_- \delta Q_W^{-(ii)} = p_- \Big[\frac{e^{-\beta_H \Delta}}{1 + e^{-\beta_H \Delta}} - \frac{2e^{-\beta_M \Delta} + 1}{3(1 + e^{-\beta_M \Delta})} \Big] \Delta. \tag{2.30}$$

The positive work condition for the three level fridge is hence given by

$$\frac{2e^{-\beta_M \Delta}+1}{3\left(e^{-\beta_M \Delta}+1\right)} > \frac{e^{-\beta_H \Delta}}{1+e^{-\beta_H \Delta}}. \tag{2.31}$$

The work cost per cycle of the three-level refrigerator is similar to that of the two-level refrigerator. This is because the measurement and erasure procedure is the same for both protocols, the only difference being that since $\beta_M < \beta_C$, p_- is slightly greater in the case of the three-level refrigerator. Since p_- is always less than one half, this results in an increase in the work cost for resetting the register according to equation (2.25).

It is evident that, for a given β_C and β_H, the three-level fridge protocol has a higher heat transfer per cycle, and a higher efficiency. Once β_M is chosen according to equation (2.27), we will have $\beta_M < \beta_C$. This implies that the working system after ICO thermalisation and $|-\rangle_c$ measurement on the control qubit, $\rho_W^{-(\mathrm{i})}$, will have a higher temperature in the case of the three-level cycle. As a consequence, more heat will be transferred to the hot reservoir during step (ii) in the case of this measurement. Furthermore, p_- is greater for lower inverse temperatures β. The magnitude of $\delta Q_C^{cycle} = p_- \delta Q_W^{-(ii)}$ is therefore greater for the three-level refrigeration cycle. This effect is more than enough to overcome the slight increase in work cost, since $p_-/\delta W_{cycle}$ is a strictly increasing function in p_-. Overall, therefore, the three-level refrigerator has a higher coefficient of performance.

2.5 Discussion

These results show that thermalisation processes happening in a world where the causal order is indefinite exhibit radically different features compared to thermalisation processes happening in a well-defined order. More broadly, they open up a new direction of research on the study of quantum thermodynamical operations enhanced by indefinite causal order. Additionally, the results are of interest for resource theories of thermodynamics, since they show that a certain thermodynamic task - the transfer of heat from a cold to a hot reservoir - can be

achieved by using thermalising channels alone, if one is allowed to apply them in an indefinite causal order (as well as measure a control qubit). This task would clearly be impossible if the channels could only be applied in a fixed or classically random order. This capability, provided by the ICO, becomes particularly relevant in the case where the control qubit cannot be used for direct thermalisation (perhaps because its states are degenerate in energy). Thus, the ICO acts as a 'tap' which allows us to access the free energy of the control qubit, which is the only source of free energy for the protocol. This free energy is made available for use by the manner in which the control qubit contols the order of the operations. It ends the process in a mixed state with reduced free energy, with the difference transferred to the other systems. The fact that it is possible to perform this task with only thermalising channels suggests the development of a new class of thermodynamic resource theories, in which operations can be performed in indefinite causal orders. It is reasonable to expect that these theories might have exotic properties that differ substantially from their counterparts with fixed casual orders.

These results demonstrate that in at least one case, a quantum uncertainty in the causal structure of a thermodynamic processes can provide a thermodynamic advantage. It is natural to believe that there might be other thermodynamic protocols that can be made possible or enhanced with the use of indefinite causal order. It is hoped that this work will encourage more investigation into new avenues utilising indefinite casual orders in thermodynamics.

Experimental realisation of refrigeration using indefinite causal orders should be achievable. Tabletop photonics experiments [19–21] have already been carried out to demonstrate enhanced communication using the quantum SWITCH. The step from these experiments to implementing the ICO refrigerator should be, in principle, not too great. An implementation of the simulation circuit should also be achievable on many other qubit platforms using current technology.

The application of the pseudo-density matrix formalism [37] to the two level system before and after its ICO interactions could provide an interesting insight into

the causal structure underlying the operation of the quantum SWITCH. This is left for future work.

Also can any understand the spreadings of the clouds?

—Job 38:37 (KJV)

3 Cloud Quantum Refrigeration

Contents

3.1 Introduction 37
3.2 Methods 40
3.3 Results 42
3.4 Noise Considerations 44
3.5 Future Circuits 46
3.6 Discussion 48

This chapter is based on a paper, written in collaboration with Felix Tennie, which is currently under review for publication in *Physical Review Letters*. The pre-print can be found on *arXiv.org* [38]. The author of this thesis designed and carried out the experiment with much helpful input from FT.

3.1 Introduction

In the previous chapter, it was demonstrated that the quantum SWITCH could be used to allow quantum refrigeration using thermalising channels that would ordinarily be useless for this task. There have been experiments aiming to implement this protocol in nuclear magnetic resonance [23] and photonic [39] systems. In this work, we implement a quantum refrigeration protocol based on the ICO

protocol, using superconducting qubits, hosted on a cloud based server which is open to all users of the internet.

The quantum SWITCH of two channels cannot be simulated with a single use of each channel embedded in a definite causal order, or in a conventional quantum circuit, without the presence of time-like curves [6]. However, by relaxing the restriction that each channel be used only once, it is possible to create a quantum circuit which gives the same output as the SWITCH. This enables a proof of principle test of the refrigeration protocol, as well as an investigation of its robustness to noise. Although this quantum circuit protocol should strictly be called a simulation of the indefinite causal order refrigerator, it is a true example of a quantum refrigerator in its own right, and its operation is closely based on and analogous to that of its progenitor.

The experimental platform that is used for the simulation is provided by IBM Quantum [40]. Since this cloud quantum computing platform was launched in 2016, it has been used to obtain several experimental results (e.g. [41–49]). There are a number of superconducting transmon qubit processors on which programs can be executed, with varying numbers of qubits and operational fidelities. Some of these quantum processors available to anyone for use, and others require affiliation with certain institutions for access. For the simulation detailed in this work, only the processors in the former category were used, illustrating the suitability, not only of currently available, but even of less than state of the art systems for the execution of the protocol.

Recall that, mathematically, the quantum SWITCH of two quantum channels is itself a quantum channel.

$$S(\mathcal{N}_1, \mathcal{N}_2)(\rho_c \otimes \rho) = \sum_{i,j} W_{ij}(\rho_c \otimes \rho)W_{ij}^\dagger,$$

where

$$W_{ij} = |0\rangle\langle 0|_c \otimes K_i^{(1)}K_j^{(2)} + |1\rangle\langle 1|_c \otimes K_j^{(2)}K_i^{(1)},$$

are the Kraus operators of the composite channel generated by the quantum SWITCH. The fact that the output of the quantum SWITCH is a quantum channel, implies that there is a unitary quantum circuit which acts on the system and an environment to give an identical output (equation 1.15).

In the previous chapter it was shown that the quantum SWITCH of two thermalising channels displays some remarkable properties. For initial $\rho_c = |+\rangle\langle+|_c$, the output of the quantum SWITCH of these channels, after measurement of the control qubit in the $|\pm\rangle_c$ basis, reads

$$ {}_c\langle\pm| S(\mathcal{N}^\tau, \mathcal{N}^\tau)(\rho_c \otimes \rho) |\pm\rangle_c = \frac{\tau}{2} \pm \frac{1}{2}\tau\rho\tau,$$

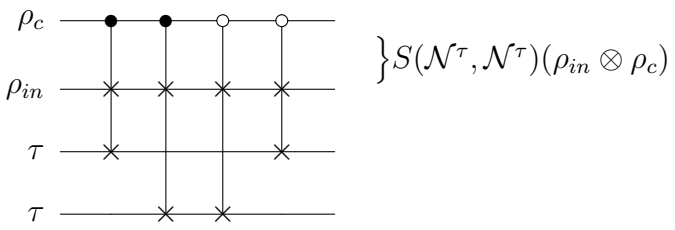
where τ is the density operator representing the thermal state which is the output of the thermalising channel $\mathcal{N}^\tau$. Note that if the channels are performed in any classically determined or random order, then the output must be τ. We see however, that this expected outcome is not obtained when the channels are applied in an indefinite causal order. Instead, the output state retains some dependence on the input, and in general will exhibit a different effective temperature than τ.

These features were used to create a thermodynamic refrigeration cycle (section 2.3) which transfers heat from cold to hot reservoirs, by thermalising a working qubit with those reservoirs in an indefinite causal order. The target system, henceforth called the working system, starts at the temperature of the two cold reservoirs. It is acted on by the quantum SWITCH of two thermalising channels, one for each reservoir. The control qubit is then measured in the $|\pm\rangle_c$ basis. If the result of the measurement yields $|+\rangle\langle+|_c$, then the working system has been cooled down. It is then thermalised classically with the cold reservoirs. If the result yields $|-\rangle\langle-|_c$, then the working system is first thermalised with the hot reservoir, and then finally with the cold reservoir. The net result of this cycle is that heat is transferred from the cold to the hot reservoir.

In order to simulate this refrigeration protocol on a quantum computer, the first step is to find a quantum circuit which gives an identical output to the output of the SWITCH of two thermalising channels.

3.2 Methods

It is possible to construct a Quantum Switch of thermalising channels using a unitary quantum circuit which acts on the control and target systems, plus environments [34]:



Here, the control qubit is represented by the uppermost wire, the working qubit by the second wire, and the two reservoir qubits by the third and fourth wires. The gates of the circuit are controlled swap operations. The target qubits, indicated by the crosses, are swapped conditional on the control qubit being in the state $|1\rangle$, for a filled circle, or $|0\rangle$, for an empty circle. The output of this circuit for the upper two qubits is identical to $S(\mathcal{N}^\tau, \mathcal{N}^\tau)(\rho \otimes \rho_c)$ above (see appendix A.1 for a derivation of this result). If the reservoir is a bath of thermal qubits, then since the Hamiltonian of the reservoir can be decomposed into a sum over the energy of each qubit, the Gibbs state of the reservoir is the product state of single qubit Gibbs states τ. The third and fourth qubits in the circuit can then be thought of as having been drawn randomly from the reservoir. Any heat flow to or from these qubits thus implies a heat flow to or from a reservoir. It is then clear that the individual swaps performed are unitary extensions of the individual quantum thermalising channels we wish to implement in the quantum SWITCH, so we implement the correct channels in an order determined by the control qubit. It is interesting to note that, after a measurement of the control qubit is made, the effective temperature of each marginal state on the reservoir wires is identical to that of the working system.

Our aim was to implement this refrigeration protocol in a physical system. We ran the experiment on the cloud quantum computing platform provided by IBM

Quantum. The quantum processors accessible via this program are comprised of superconducting transmon qubits [50, 51].

Specifically, we used the *ibmq_5_yorktown* backend (figure 3.1), which is one of the IBM Quantum Canary Processors. The processor consists of 5 transmon qubits, and possesses a universal gate set with high connectivity (six out of ten potential couplings are possible) and relatively high fidelity, and so is ideally suited for our purpose.

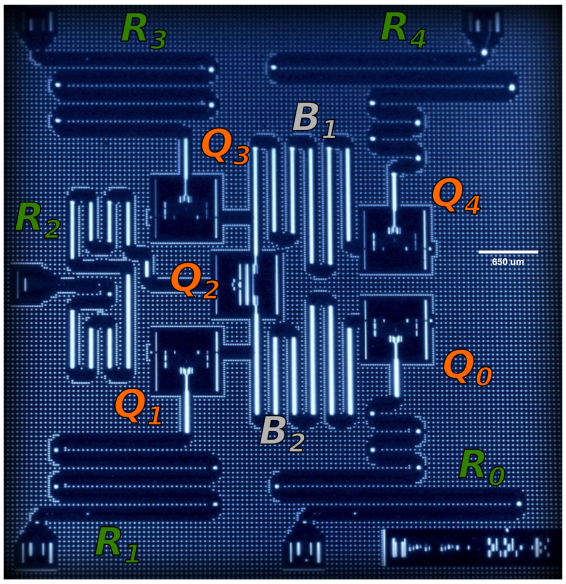
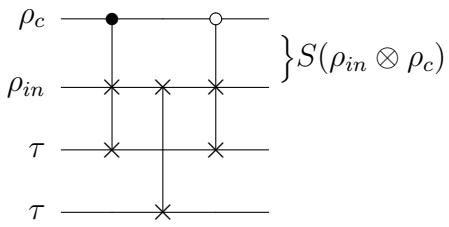


Figure 3.1: Image of the IBM Quantum *yorktown* canary processor, taken from the readme documentation. Q_{0-4} label the transmon qubits, R_{0-4} the readout resonators, and B_{1-2} the bus resonators coupling Q_2, Q_3, Q_4 and Q_0, Q_1, Q_2 respectively.

It is important that the circuit be reduced and simplified as much as possible, to improve the overall fidelity. We first notice that the circuit above can be simplified using circuit identities to become:



The (controlled) swap gates can be decomposed into Toffoli and C-NOT gates. The circuit is then transpiled using the native IBMq transpiler for the allowed operations and connectivity of the particular backend which has been selected for the experiment. The depth of the final transpiled circuit is 31. The circuit consists of 51 gates, of which 19 are two qubit gates. These two qubit gates have a higher error by an order of magnitude, so care is taken to minimise the number of such gates in the circuit.

The control qubit is initialised in the state $|+\rangle_c$. The refrigeration protocol requires that the work and reservoir qubits are initialised in thermal mixed states, all at the same inverse temperature, β_{in}. In order to achieve this, we run the circuit 40960 times[1] with each possible computational basis state for the thermal qubits. One example outcome for a particular input basis state is shown in Fig. 3.3. The desired input mixed state is created by randomly selecting runs with a weighting for each input state that depends on the desired input state. Simply by including a fifth qubit representing a hot reservoir and relabelling the qubits depending on the measurement result of the control qubit, we can then reproduce the two level refrigeration cycle presented in section 2.4.1. The data were analysed by separating the runs according to the measurement result for the control qubit and then summing over both results of all the qubits except the qubit of interest. This gives an average output temperature for the working system and reservoir qubits.

3.3 Results

Our results demonstrate that non-classical cooling has been achieved. For a range of input temperatures, we find that the reservoir and working qubits have been cooled below their common input temperature. In accordance with the theoretical predictions detailed above, we find that the temperature of the thermal qubits is correlated with the state of the control qubit - something that is not consistent with the channels being applied in any classical order, thus demonstrating the

[1] This reduces the sampling error to an acceptable level. The precise number is the result of the options for number of runs provided by IBMq.

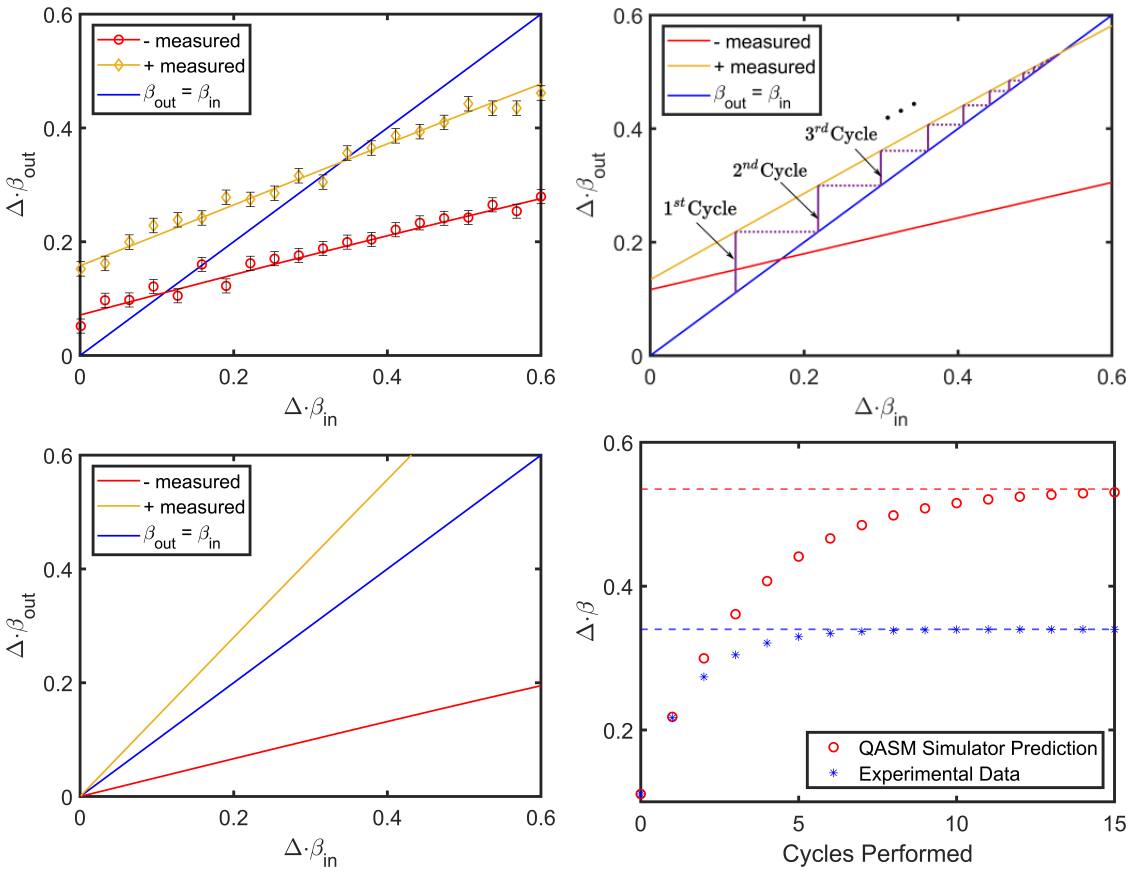


Figure 3.2: Dimensionless inverse temperature of the working qubit after thermalisation in an indefinite causal order, plotted as a function of input temperature. The blue line represents the outcome in the classical case - the channels are performed in a definite causal order and so there is no change in temperature. The yellow line is the output temperature when the control qubit is measured to be $|+\rangle$. In this case, for all input temperatures, the output is cooler than the case when the control is found in the state $|-\rangle$ (red line). *Top Left* – Experimental Result. *Top Right* – QASM noise model simulation with IBMq backend calibration data. Solid and dashed line represents ideal temperature trajectory over multiple cycles with measurement result $|+\rangle$. *Bottom Left* – Noiseless theoretical prediction. *Bottom Right* – Dimensionless inverse temperature as a function of the number of consecutive cycles with measurement result $|+\rangle$. The temperature converges to an asymptote (blue dashed line for experiment, red dashed line for noise model simulation).

crucial role of indefinite causal order in the cooling process. For a given range of input temperatures, we observe that the thermal qubits are cooled below the input temperature when the control qubit is found in the state $|+\rangle_c$, and are heated above the input temperature when it is found in state $|-\rangle_c$, as shown in Fig. 3.2. This presents a clear signature that quantum refrigeration has been performed.

In the noiseless case, the lower bound on the temperature to which the qubits

can be cooled by the protocol is absolute zero. Our results, however, indicate that there is a temperature, below which the qubits cannot be cooled. This is a result of the inherent temperature of the noise associated with the operations performed. This temperature bound can be read off the graph in Fig. 3.2 (Top Left), from the point where the line representing the output temperature when $|+\rangle_c$ is measured crosses the line $\beta_{\text{out}} = \beta_{\text{in}}$. For the IBMq Yorktown backend that was used, the inverse temperature bound was given by $\Delta \cdot \beta \approx 0.3$, where Δ is the energy gap of the qubits. It is also possible to infer from our results the minimum number of cycles necessary to cool all the thermal qubits by a certain temperature (Fig. 3.2, Bottom Right), in the ideal case where $|+\rangle_c$ is measured each time (and thus no thermalisation with a hot reservoir is required). This is a lower bound on the number of cycles which must be performed. More generally, the expected number of cycles depends on p_+ and p_- (the probability of measuring $|+\rangle_c$ and $|-\rangle_c$ respectively). For the relevant temperature ranges, it is reasonable to take $p_+ \approx p_- \approx 1/2$. Then, the expected number of cycles required will be approximately 2^n, where n is the number of steps required in the ideal case.

3.4 Noise Considerations

A close examination of the data presented in Fig. 3.2 reveals a number of unexpected features that warrant further discussion. In particular, let us consider the outputs in the regime where the input inverse temperature is very low ($\beta_{\text{in}} \to 0$). First, we observe that the experimental data (Top Left) shows that for low β_{in} the temperature of the working system is decreased for both possible measurements of the control qubit. Also, the temperature depends on the result of this measurement, whereas in the theoretical model (Bottom Left), for $\beta_{\text{in}} = 0$, we have $\beta_{\text{out}} = 0$, for both $|+\rangle_c$ and $|-\rangle_c$ measurements. The first feature of the data can be understood with reference to a very simple model of the noise associated with the operations of the computer. In this model, we assume that there are two possible outcomes of the process. With some probability, the computer operates perfectly and gives the theoretically expected output for a given input temperature, $\rho_{th}(\beta_{\text{in}})$, otherwise, the

output is a fixed density matrix ρ_{fail}. We calculate the 'success probability' (p_{suc}) by multiplying together the fidelities (from the backend calibration data) of each of the quantum gates and measurements performed. The output then takes the form

$$\rho_{out} = p_{suc}\ \rho_{th}(\beta_{\text{in}}) + (1 - p_{suc})\rho_{fail}. \tag{3.1}$$

The form of ρ_{fail} is unknown (the error processes can be represented by some combination of depolarising and dephasing channels), but since the off-diagonal elements are unimportant, there is only one parameter relevant to the model: the effective temperature of the state. Since this effective temperature will be finite, and p_{suc} is less than unity, $\beta_{\text{out}} = 0$ can never be achieved, even when $\beta_{\text{in}} = 0$. However, this model does not explain why, when β_{in} is very low, β_{out} depends on the measurement results ($|+\rangle_c$ or $|-\rangle_c$) of the control qubit. In fact, the model above (Eq. 3.1) predicts that there will be no splitting in output temperature when $\beta_{\text{in}} = 0$.

A simple modification to the model can explain this second feature of the data. Let us assume that the input states of the process are not perfectly prepared, but rather are prepared correctly with a certain probability, and otherwise are initialised in some thermal state of unknown temperature. Thus, the effective temperature of the input states cannot be controlled precisely. It is therefore clear that the input states will never have a temperature of exactly $\beta_{\text{in}} = 0$. Therefore, ρ_{th} in Eq. (3.1) must be replaced with

$$\rho'_{th}(\beta_{\text{in}}) = p'_{suc}\ \rho_{th}(\beta_{\text{in}}) + (1 - p'_{suc})\rho_{th}(\beta_{\text{fail}}),$$

where p'_{suc} is the probability of a faithful initialisation and β_{fail} is the temperature of the input when the initialisation fails. Since β_{fail} is a finite temperature, with ρ'_{th} we still expect a splitting of β_{out} for the $|+\rangle_c$ and $|-\rangle_c$ measurement results.

A more sophisticated noise model, provided by IBM Quantum, with parameters specific to the quantum backend used, gives a more accurate picture of the noise processes which occur. This model includes sources of error such as single qubit operation errors, readout errors and errors associated with C-NOT operations. We provide a sample histogram (Fig. 3.3) for comparison between the measured data

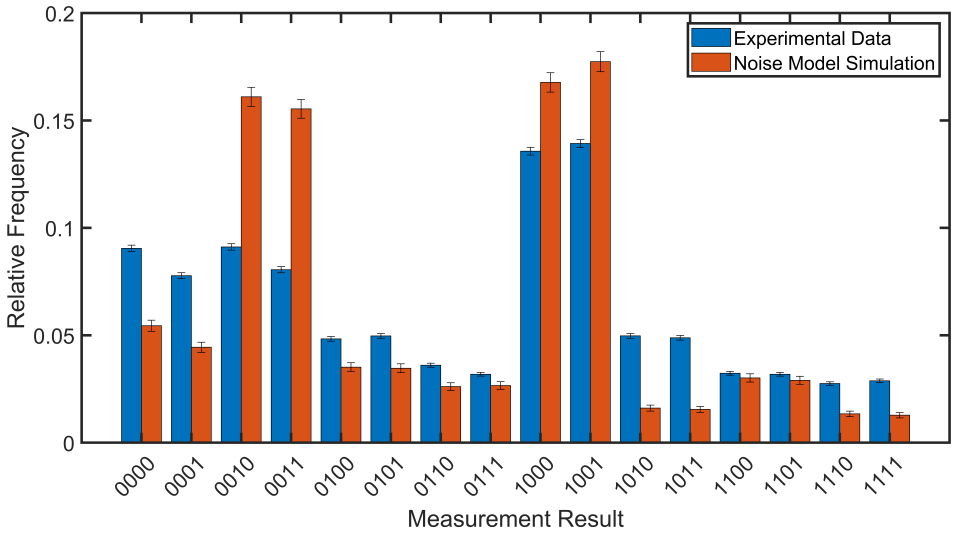
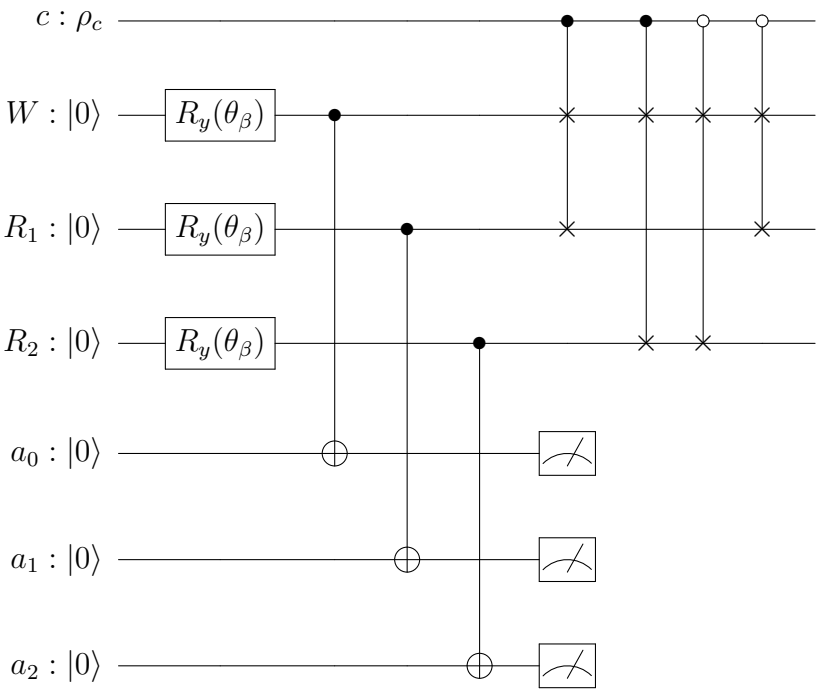


Figure 3.3: Histogram of the output measurement results for a particular input computational basis state (in this case work qubit '1', reservoir A '0' and reservoir B '0'). The measurement outcome labels on the horizontal axis have bits which correspond to, from least to most significant bit: control qubit, reservoir A, work qubit, reservoir B. *Left, Blue* – Experimental Result. *Right, Red* – QASM Noise Model Prediction. It is easily observed that the result is not compatible with the noise model within statistical error. This indicates the presence of correlated noise which is not accounted for in the model.

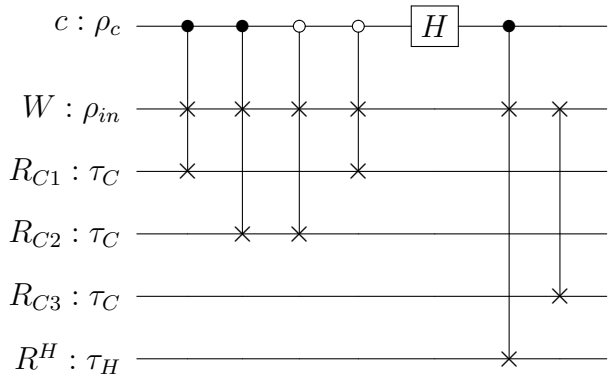
(blue) and this model's prediction (red). These data arise from a particular input computational basis state of the thermal qubits. Still, there is a deviation of the measured data, even from this comprehensive noise model, which cannot be resolved within the bounds of sampling errors. This inaccuracy may arise because, either the calibration data were not accurate for the time that the experiment took place, or because of unknown and unaccounted sources of correlated noise.

3.5 Future Circuits

As the fidelities of quantum information systems improve, variants of the circuit described in this chapter will become possible which make certain steps of the thermodynamic procedure more explicit. For example, it might be desired that the mixedness of the initial states entering the circuit be generated by some other means, besides the post-processing step of collating runs of the experiment based on a weighting corresponding to the desired input temperature.



This circuit achieves a mixedness for the input via entanglement and quantum measurement. The gates $R_y(\theta_\beta)$ are rotations about the y-axis of the Bloch sphere by an angle θ_β which is determined by the desired input temperature. Once the auxiliary qubits a_0, a_1, a_2 are measured, and the results discarded, the states of the work and reservoir qubits W, R_1, R_2 respectively will be projected into the desired random mixed states. Another improvement on the circuit implemented in this chapter would be one which implements every step in the refrigeration cycle explicitly, without the need for relabelling qubits. Such a circuit is given below:



This circuit simulates every step of the refrigeration protocol of section 2.4.1. R_{C1-3} are 3 qubits drawn randomly from the cold reservoir, and R_H is a qubit drawn randomly from the hot reservoir. The first four controlled swaps implement step (i). The Hadamard gate along with the fifth control swap gate implements step (ii) — if the control qubit is in the state $|-\rangle_c$ then the working system is thermalised with the hot reservoir. Step (iii) is performed by the last swap gate which thermalises the working system with the cold reservoir and returns it to its initial state. At the end of the cycle the reservoir qubits are returned to the appropriate reservoirs. To perform the cycle again the control qubit must be reset and new reservoir qubits drawn.

3.6 Discussion

As far as the author is aware, this work, together with Ref. [23], constitutes the first refrigeration cycle run on a programmable quantum computer. It has been shown that current quantum processors can be used to successfully implement such protocols, and provide a new test bed for quantum thermodynamics.

The implementation of the quantum SWITCH on a quantum computer allows for easy generalisation and extension of any ICO protocol. For example, it is possible to choose any desired input state of the control qubit, and any channels to place in a superpostion of orders. It is also possible to straightforwardly extend the SWITCH to $N > 2$ channels and orders. This permits a full investigation of the advantage provided by the quantum SWITCH.

The experiment is a proof of principle of the indefinite causal order refrigeration cycle. A very simple model of the noise which explains the major features of the observed data, as well as a more sophisticated one, capable of reproducing the key features of the data, have been presented. The successful implementation of the cycle in a noisy system proves the robustness of the protocol, and indicates that other ICO protocols need not necessarily be rendered impotent on account of noise. Further understanding the impact of noise on ICO-enhanced tasks is essential to

evaluating the full potential of the quantum SWITCH for applications not limited to thermodynamics, but also including communication and metrology. These results are a promising indicator for the robustness of ICO protocols to noise.

This work motivates further research on the limitations of the quantum SWITCH in assisting thermodynamic tasks, and the search for other, perhaps more efficient, (refrigeration) protocols. One open question is whether it is possible to realise an ICO thermodynamic cycle whose efficiency can, in principle, approach Carnot efficiency. It is likely that this might be possible using a modified version of the cycle implemented here.

It has been demonstrated that a thermodynamic ICO protocol can be implemented using current technology. The search is on for more such protocols, and the prospect for their physical realisation is very encouraging.

People talk about this being an uncertain time. You know, all time is uncertain.

—Warren Buffett (Crippen, 2010)

4

Indefinite Causal Order from Superpositions in Time

Contents

4.1 Introduction 52
4.2 Formalism for Quantum Events 53
4.3 Deriving ICO from Superpositions in Time 55
4.4 Strategies for a Quantum SWITCH via Time Superpositions 59
4.4.1 Via Time-Bin Entanglement 59
4.4.2 Via Decaying Atoms 60
4.4.3 Alternative Derivation for Decaying Atoms protocol . . 61
4.5 Discussion 64

This chapter is based on a paper, written in collaboration with Nicetu Tibau Vidal and Eduardo Dias, which is yet to be published. The pre-print can be found on *arXiv.org* [52]. The author of this thesis was responsible for the initial idea for the project, while ED is the creator of the time superposition formalism. NV helped to solve many problems along the way.

4.1 Introduction

A growing literature has arisen describing events that take place without a well defined causal structure in quantum mechanics [4–6, 8, 16, 18–21, 26–31, 34]. On the one hand, these works are motivated by the hypothesis that an eventual quantum theory of gravity might predict superpositions of spacetime geometries, in which the causal relationship between events is itself in a superposition [4]. On the other hand, it has been argued that indefinite causal orders (ICOs) can be found already within traditional quantum mechanics, without the need for superpositions of spacetime geometries [16, 18–21, 27].

In this thesis, the main example of an indefinite causal structure we have considered is the quantum SWITCH, in which an auxiliary degree of freedom controls coherently the order in which operations act on system. The quantum SWITCH is a higher order quantum operation that cannot be represented exactly using a standard quantum circuit [6]. As already discussed, the quantum SWITCH has been shown to provide advantages in quantum computation [26, 27], communication [28–30], metrology [31–33], and, as previously described, quantum refrigeration [34]. Considering these many useful applications of the quantum SWITCH, a relevant question is how this higher order operation might be realised, and the resources which are required for this realisation. The demonstration of the use of the quantum SWITCH, has been claimed in recent experiments [16, 18–21] using tabletop photonics. There is however some debate about whether these experiments exhibit a true ICO.

In this chapter, we obtain ICOs from the natural uncertainty regarding the moment at which two events A and B occur, e.g., the detection of spontaneous decays or the arrival of particles in an apparatus. We couple this uncertainty in a precise way, such that the quantum SWITCH of operations U_A and U_B is implemented on a system $\mathcal{S}$. Thus, without resorting to unknown high-energy quantum gravitional effects, we provide a scheme in which U_A and U_B act in a temporal superposition that encompasses both possibilities "U_A acting before U_B"

and "U_B acting before U_A." These unitary operations can also be thought of as extensions of quantum channels in an ICO.

4.2 Formalism for Quantum Events

Although in this work we deal with the Schrödinger prescription of QM, where a time coordinate tracks the evolution of the system, we treat the instant of time when an event occurs as an observable. In this context, we will take advantage of certain aspects of an approach developed recently [53], where a space-time-symmetric formalism for events is proposed, to compute a quantum state with indefinite causal orders. The formalism is used to describe measurements on a system $\mathcal{Q}$, using a timer $\mathcal{T}$, which is coupled to a detector $\mathcal{D}$. The detector performs a measurement of the observable $\alpha = \sum_\alpha \alpha \left|\alpha\right\rangle \left\langle\alpha\right|_\mathcal{Q}$ of the system. We consider first the interaction of the detector with the system. The initial combined state is given by

$$\left|\psi_i\right\rangle_{\mathcal{QD}} = \left|0\right\rangle_\mathcal{Q} \otimes \left|0\right\rangle_\mathcal{D} = \sum_\alpha \left\langle\alpha|0\right\rangle_\mathcal{Q} \left|\alpha\right\rangle_\mathcal{Q} \otimes \left|0\right\rangle_\mathcal{D}, \tag{4.1}$$

where $\left|0\right\rangle_\mathcal{Q}$ is the initial state of the system and $\left|0\right\rangle_\mathcal{D}$ that of the detector. Once the detection has taken place, then the overall state of the system can be written

$$\left|\psi_f\right\rangle_{\mathcal{QD}} = \sum_\alpha \left\langle\alpha|0\right\rangle_\mathcal{Q} \left|\alpha\right\rangle_\mathcal{Q} \otimes \left|\alpha\right\rangle_\mathcal{D}. \tag{4.2}$$

For our purposes, we would like to be able to describe events which happen at a time which is subject to quantum uncertainty, so let us consider the timer system which records the moment of the detector's measurement. We represent $\mathcal{T}$ as a Salecker-Wigner-Peres-like timer [54, 55], in which an ideal quantum clock, coupled with the detector $\mathcal{D}$, stops running at the moment of detection. The initial state of the systems is thus

$$\left|\psi(t_0)\right\rangle_{\mathcal{QDT}} = \left|0\right\rangle_\mathcal{Q} \otimes \left|0\right\rangle_\mathcal{D} \otimes \left|t_0\right\rangle_\mathcal{T} = \sum_\alpha \left\langle\alpha|0\right\rangle_\mathcal{Q} \left|\alpha\right\rangle_\mathcal{Q} \otimes \left|0\right\rangle_\mathcal{D} \otimes \left|t_0\right\rangle_\mathcal{T}. \tag{4.3}$$

We break up the subsequent evolution into infinitesimal time steps which are much shorter than the other relevant time scales of the process. Here, unlike in

Ref. [53], we will assume, for the sake of simplicity, that the system $\mathcal{Q}$ has a zero Hamiltonian and hence does not evolve while isolated. After the first such step the state of the systems becomes

$$|\psi(t_1)\rangle_{\mathcal{QDT}} = \sqrt{1-\delta p_{(1)}}\; e^{i\phi_1} \sum_\alpha \langle\alpha|0\rangle_{\mathcal{Q}} |\alpha\rangle_{\mathcal{Q}} \otimes |0\rangle_{\mathcal{D}} \otimes |t_1\rangle_{\mathcal{T}} + \sqrt{\delta p_{(1)}} \sum_\alpha \langle\alpha|0\rangle_{\mathcal{Q}} |\alpha\rangle_{\mathcal{Q}} \otimes |\alpha\rangle_{\mathcal{D}} \otimes |t_1\rangle_{\mathcal{T}}\,. \tag{4.4}$$

In the second line of this expression, with probability δp_1, the detection has taken place, and so the detector records a value for α and the timer stops ticking, recording the time t_1. In the first line the detection has not taken place, so the detector remains in its initial state, and the timer continues ticking. This term in general has some phase ϕ_1 relative to the second. After N such steps the state is given by

$$|\psi(t_N)\rangle_{\mathcal{QDT}} = \Gamma_A(t_N,t_0) \sum_\alpha \langle\alpha|0\rangle_{\mathcal{Q}} |\alpha\rangle_{\mathcal{Q}} \otimes |0\rangle_{\mathcal{D}} \otimes |t_N\rangle_{\mathcal{T}} + \sum_{k=1} \tilde{\chi}(t_k) \sum_\alpha \langle\alpha|0\rangle_{\mathcal{Q}} |\alpha\rangle_{\mathcal{Q}} \otimes |\alpha\rangle_{\mathcal{D}} \otimes |t_k\rangle_{\mathcal{T}}\,, \tag{4.5}$$

where

$$\Gamma_A(t_N,t_0) = \prod_{k=1}^{N} \sqrt{1-\delta p_{(k)}}\; e^{i\phi_k}, \tag{4.6}$$

and

$$\tilde{\chi}(t_k) = \sqrt{\delta p_{(k)}} \prod_{l=1}^{k-1} \sqrt{1-\delta p_{(l)}}\; e^{i\phi_l}. \tag{4.7}$$

The first line of expression (4.5) represents the case in which, after N time steps, the detection has still not occurred. The second line is a sum over all possible detection time steps. Inspecting this expression, we see that the uncertainty in time of the detection has led to a superposition of these times, which is reflected in the superposition of different states of the timer $\mathcal{T}$. In [53], the author goes on to consider multiple events and examine how a succession of such events, associated

with an observer (a collection of timers and detectors), can give rise to the bottom-up emergence of time, by incorporating elements of the Page-Wootters formalism [56]. However, the possibility for events to occur in non-predetermined orders was not explored, and, as we will see, the approach detailed above can be fruitfully applied to such situations. We will thus extend it by allowing events to occur in different orders, and by allowing the detections which occur to trigger operations on other systems. With these extensions we will be able to describe the emergence of indefinite causal orders, and specifically, the quantum SWITCH.

4.3 Deriving ICO from Superpositions in Time

For the sake of clarity, we will show how indefinite causal orders can arise in a simple situation in which the decays of two uncorrelated atoms take place in a superposition of temporal orders. Consider the spontaneous emission of two atoms $\mathcal{S}_A$ and $\mathcal{S}_B$ with decay rates γ_A and γ_B, respectively. The emitted photons from $\mathcal{S}_A$ and $\mathcal{S}_B$ trigger the unitary operations $U_A \otimes H$ and $U_B \otimes \sigma_z$ to act jointly on the system ($\mathcal{S}$) and the control qubit ($\mathcal{C}$), via a machine $\mathcal{M}$. Here, H and σ_z are the Hadamard and the Pauli-z matrix in the basis $\{|0\rangle_\mathcal{C}, |1\rangle_\mathcal{C}\}$, respectively. $\mathcal{M}$ registers the instant that the photons were received and performs their respective unitaries. To this end, the machine can have (among other subsystems) internal timers, such as the Salecker-Wigner-Peres-like timer $\mathcal{T}$, where the clock stops running when $\mathcal{M}$ detects the decay $\mathcal{S}_A$ or $\mathcal{S}_B$. We assume that the operations take place instantaneously and that the free evolution of the system $\mathcal{S}$ and control $\mathcal{C}$ is the identity.

The system starts in the state

$$|\psi(t_0)\rangle = |e,e\rangle_{AB}\ |0,0\rangle_\mathcal{M}\ |+\rangle_\mathcal{C}\ |\varphi\rangle_\mathcal{S}, \tag{4.8}$$

where $|e,e\rangle_{AB}$ are the excited states of $\mathcal{S}_A$ and $\mathcal{S}_B$, and $|0,0\rangle_\mathcal{M}$ is the ready state of $\mathcal{M}$'s degrees of freedom that register the two different instants at which the operations take place. $|\varphi\rangle_\mathcal{S}$ is the initial state of $\mathcal{S}$ and $|+\rangle_\mathcal{C} = (|0\rangle_\mathcal{C} + |1\rangle_\mathcal{C})/\sqrt{2}$ is chosen as the ready state of the control qubit. To prevent a dense notation, we avoid using the symbol $\otimes$. Let us calculate $|\psi(t)\rangle$ by breaking up the Schrödinger

evolution into infinitesimal steps $\delta t = t_{k+1} - t_k \ll 1/\gamma_j$ $(k = 1, 2, \ldots)$ in such a way that after the first step of the evolution, the initial state (4.8) has evolved to

$$\begin{aligned}|\psi(t_1)\rangle = &\sqrt{1-\delta p_A}\sqrt{1-\delta p_B}\;|e,e\rangle_{AB}\;|0,0\rangle_{\mathcal{M}}\;|+\rangle_{\mathcal{C}}\;|\varphi\rangle_{\mathcal{S}} \\ &+\sqrt{\delta p_A}\sqrt{1-\delta p_B}\;|g,e\rangle_{AB}\;|t_1,0\rangle_{\mathcal{M}}\;|0\rangle_{\mathcal{C}}\;U_A\;|\varphi\rangle_{\mathcal{S}} \\ &+\sqrt{1-\delta p_A}\sqrt{\delta p_B}\;|e,g\rangle_{AB}\;|0,t_1\rangle_{\mathcal{M}}\;|-\rangle_{\mathcal{C}}\;U_B\;|\varphi\rangle_{\mathcal{S}},\end{aligned} \tag{4.9}$$

with $\delta p_j = \gamma_j \delta t \ll 1$ being the probability of detecting the emission of $\mathcal{S}_j$ in the interval δt. This ensures that the time step used is short enough such that we can neglect the probability $\delta p_A \delta p_B$ of both events A and B (detections of $\mathcal{S}_A$ and $\mathcal{S}_B$ decays) happening simultaneously.

In the first line of the expression for $|\psi(t_1)\rangle$, we verify that with a high probability $(1-\delta p_A)(1-\delta p_B)$, A and B do not take place (U_A and U_B are not triggered), and hence the machine and the control qubit remain in their initial states. In the next lines, with probability $\delta p_A(1-\delta p_B)$ $[\delta p_B(1-\delta p_A)]$, $\mathcal{S}_A$ $[\mathcal{S}_B]$ decays, and thus $U_A \otimes H$ $[U_B \otimes \sigma_z]$ acts on $\mathcal{S} \otimes \mathcal{C}$. The machine registers t_1 in different degrees of freedom, depending on which operation is applied.

Calculating this evolution up to the N-th step, we have

$$\begin{aligned}|\psi(t_N)\rangle = &\;\Gamma_A(t_N,t_0)\;\Gamma_B(t_N,t_0)\;|e,e\rangle_{AB}\;|0,0\rangle_{\mathcal{M}}\;|+\rangle_{\mathcal{C}}\;|\varphi\rangle_{\mathcal{S}} \\ &+\Gamma_B(t_N,t_0)\sum_{k=1}^{N}\tilde{\chi}_A(t_k,t_{k-1})\;|g,e\rangle_{AB}\;|t_k,0\rangle_{\mathcal{M}}\;|0\rangle_{\mathcal{C}}\;U_A\;|\varphi\rangle_{\mathcal{S}} \\ &+\Gamma_A(t_N,t_0)\sum_{k=1}^{N}\tilde{\chi}_B(t_k,t_{k-1})\;|e,g\rangle_{AB}\;|0,t_k\rangle_{\mathcal{M}}\;|-\rangle_{\mathcal{C}}\;U_B\;|\varphi\rangle_{\mathcal{S}} \\ &+\sum_{\ell=k+1}^{N}\sum_{k=1}^{N-1}\tilde{\chi}_B(t_\ell,t_{\ell-1})\;\tilde{\chi}_A(t_k,t_{k-1})\;|g,g\rangle_{AB}\;|t_k,t_\ell\rangle_{\mathcal{M}}\;|0\rangle_{\mathcal{C}}\;U_B\;U_A\;|\varphi\rangle_{\mathcal{S}} \\ &+\sum_{\ell=k+1}^{N}\sum_{k=1}^{N-1}\tilde{\chi}_A(t_\ell,t_{\ell-1})\;\tilde{\chi}_B(t_k,t_{k-1})\;|g,g\rangle_{AB}\;|t_\ell,t_k\rangle_{\mathcal{M}}\;|1\rangle_{\mathcal{C}}\;U_A\;U_B\;|\varphi\rangle_{\mathcal{S}},\end{aligned} \tag{4.10}$$

where,

$$\Gamma_j(t_N, t_0) = (1 - \delta p_j)^{N/2} \tag{4.11}$$

is the probability amplitude for the system $\mathcal{S}_j$ not to decay in the interval $[t_0, t_N]$, and

$$\tilde{\chi}_j(t_k, t_{k-1}) = \sqrt{\delta p_j}\ (1 - \delta p_j)^{(k-1)/2} \tag{4.12}$$

is the probability amplitude for $\mathcal{S}_j$ to decay in the interval $[t_{k-1}, t_k]$. Here, we assume that δp_j is the same for all intervals, but the generalisation when this is not the case is straightforward. We have also ignored the phases of equation 4.7, which are not important in what follows.

In the first line of equation (4.10), we verify that A and B do not happen in the interval $[t_0, t_N]$, thus $\mathcal{M}$ remains in the initial state. In contrast, in the second (third) line, A (B) takes place in the interval $[t_{k-1}, t_k]$, $\mathcal{M}$ registers t_k in its first (second) degree of freedom, and $\mathcal{S}_B$ ($\mathcal{S}_A$) remains in the excited state. Finally, $\mathcal{S}_A$ and $\mathcal{S}_B$ are in the ground state in the fourth (fifth) line, with $\mathcal{S}_A$ ($\mathcal{S}_B$) decaying at the instant t_k, $\mathcal{S}_B$ ($\mathcal{S}_A$) decaying later at the instant t_ℓ, and $\mathcal{M}$ registering t_k and t_ℓ.

We are interested in $|\psi(t)\rangle$ from the moment we can guarantee that both detections A and B have indeed occurred, and hence both U_A and U_B have acted on $\mathcal{S}$. We therefore evaluate $|\psi(t_N)\rangle$ when $t_N \gg t_0 + \max(1/\gamma_A, 1/\gamma_B)$, so that $\Gamma_j(t_N, t_0) \approx 0$. For simplicity, let us take $t_N \to \infty$. In this scenario, as the atoms $\mathcal{S}_A$ and $\mathcal{S}_B$ are no longer correlated to the other systems, the state of $\mathcal{MSC}$ [$|\psi\rangle \equiv |\psi(t_N \to \infty)\rangle$] in the continuous limit becomes

$$\begin{aligned} |\psi\rangle_{\mathcal{MSC}} = \int_{t_0}^{\infty}\int_{t_0}^{\infty} dt_A dt_B\ \chi_{AB}(t_A, t_B)\ |t_A, t_B\rangle_{\mathcal{M}} \\ \otimes\Big[\Theta(t_B - t_A)\ |0\rangle_{\mathcal{C}}\ U_B\ U_A\ |\varphi\rangle_{\mathcal{S}} \\ +\Theta(t_A - t_B)\ |1\rangle_{\mathcal{C}}\ U_A\ U_B\ |\varphi\rangle_{\mathcal{S}}\Big], \end{aligned} \tag{4.13}$$

where $\chi_{AB}(t_A, t_B) = \chi_A(t_A)\chi_B(t_B)$ is the continuous versions of $\tilde{\chi}$, and $\Theta(t_x - t_y) = 1$ for $t_x > t_y$, and 0 otherwise. Besides the indefinite causal order between U_A and U_B, $|\psi\rangle_{\mathcal{MSC}}$ contains a superposition of all possible instants t_A and t_B (with weight $\chi_{AB}(t_A, t_B)$) at which U_A and U_B can act on $\mathcal{S}$.

To obtain $\chi_j(t_j)$, notice that the probability for $\mathcal{S}_j$ to decay in the interval $[t_k, t_{k+1}]$ can be calculated either by $\tilde{\chi}_j(t_k, t_{k+1})$ squared (equation (4.12)) or by the modulus square of $\chi_j(t_j)$ at the instant t_k multiplied by δt. By equating these two expressions, as $\delta p_j \ll 1$, we have

$$\delta p_j \; (k-1)\delta p_j \approx |\chi_j(t_k)|^2 \; \delta t. \tag{4.14}$$

Then, since δp_j is time-independent, let us take $\delta p_j = \gamma_j \delta t$. By considering $t_k - t_0 = k\delta t$ and isolating $|\chi_j(t_k)|^2$ in equation (4.14), we obtain that the probability density amplitude for $\mathcal{S}_j$ to decay at the instant t_j can be written as

$$\chi_j(t_j) = \sqrt{\gamma_j} \; \mathrm{e}^{-\gamma_j (t_j - t_0)/2} \tag{4.15}$$

for $t_j \geq t_0$, and $\chi_j(t_j) = 0$ otherwise.

It is worth noticing that since we chose a time-independent δp_j, $\chi_j(t_j)$ is simply the time derivative of the traditional spontaneous decay amplitude. Also, one can verify that for more complex events — where, for instance, the events associated with $\mathcal{S}_A$ and $\mathcal{S}_B$ are correlated — $|\psi\rangle_{\mathcal{MSC}}$ has the same format as equation (4.13), but with a non-separable time probability amplitude $\chi_{AB}(t_A, t_B)$.

It is evident that the superposition in equation (4.13) contains branches in which decay A happens first and U_A acts first and branches in which decay B happens first and U_B acts first. The causal order in this situation is thus indefinite. However, we have not yet recovered the mathematical form of the quantum SWITCH, because the final state of the system $\mathcal{S}$ and control $\mathcal{C}$ are still entangled with the machine $\mathcal{M}$, and depend on the distribution χ_{AB}. Nevertheless, by including $\mathcal{C}$ and $\mathcal{M}$ as part of a composite subsystem $\mathcal{C}'$, and defining the states

$$|0\rangle_{\mathcal{C}'} = \sqrt{2} \int_{t_0}^{\infty} dt_A \int_{t_A}^{\infty} dt_B \; \chi_{AB}(t_A, t_B) \; |t_A, t_B\rangle_{\mathcal{M}} |0\rangle_{\mathcal{C}} \tag{4.16}$$

and

$$|1\rangle_{\mathcal{C}'} = \sqrt{2} \int_{t_0}^{\infty} dt_B \int_{t_B}^{\infty} dt_A \; \chi_{AB}(t_A, t_B) \; |t_A, t_B\rangle_{\mathcal{M}} |1\rangle_{\mathcal{C}}, \tag{4.17}$$

equation (4.13) acquires, in principle, the mathematical structure of the action of the quantum SWITCH of U_A and U_B,

$$|\psi\rangle_{\mathcal{C}'\mathcal{S}} = \frac{1}{\sqrt{2}}\Big(|0\rangle_{\mathcal{C}'}\ U_B U_A\ + |1\rangle_{\mathcal{C}'}\ U_A U_B\ \Big) |\varphi\rangle_{\mathcal{S}}\,, \tag{4.18}$$

with $\langle 0|1\rangle_{\mathcal{C}'} = 0$ and $\langle 0|0\rangle_{\mathcal{C}'} = \langle 1|1\rangle_{\mathcal{C}'} = 1$. Note that for $|\psi\rangle_{\mathcal{C}'\mathcal{S}}$ to be the output of a usable quantum SWITCH, one should be able to distinguish between the states $|0\rangle_{\mathcal{C}'}$ and $|1\rangle_{\mathcal{C}'}$, as well as measure these systems in the complimentary basis. If this is not possible (perhaps because these systems are too complex), or if a control system which involves only a single qubit is required, then it is necessary to disentangle $\mathcal{M}$ and $\mathcal{C}$. We proceed to consider two physical realisations which are engineered such that the original quantum SWITCH is recovered.

4.4 Strategies for a Quantum SWITCH via Time Superpositions

4.4.1 Via Time-Bin Entanglement

For the first strategy, we consider a timer state that describes time-bin entangled photons, such as the ones produced in Refs. [57, 58]: $|\varphi\rangle_{AB} = \frac{1}{\sqrt{2}}\left(|e\rangle_A |l\rangle_B + |l\rangle_A |e\rangle_B\right)$. For our purposes, such states can be considered to be superpositions in time with the labels e and l denoting early (forward photon) and late (backward photon). Considering that the time-bin entangled photons ($\mathcal{S}_A$ and $\mathcal{S}_B$) trigger the operations U_A and U_B via the machine $\mathcal{M}$ as previously discussed, the time probability amplitude of Eqs. (4.16) and (4.17) is then given by $|\chi_{AB}(t_A, t_B)|^2 = \frac{1}{2}\Big[\delta(t_A - t_e)\delta(t_B - t_l) + \delta(t_A - t_l)\delta(t_B - t_e)\Big]$, where t_e and t_l are the early and late times respectively. Then, there is a superposition of operation A happening at time t_e then operation B at time t_l, and of operation B happening at time t_e then operation A happening at time t_l. Performing the integration from Eqs. (4.16) and (4.17), we obtain

$$|0\rangle_{\mathcal{C}'} = |t_e, t_l\rangle_{\mathcal{M}}\ |0\rangle_{\mathcal{C}}\ \text{ and }\ |1\rangle_{\mathcal{C}'} = |t_l, t_e\rangle_{\mathcal{M}}\ |1\rangle_{\mathcal{C}}. \tag{4.19}$$

Notice that in the particular case of this first strategy, we can neglect $\mathcal{C}$, since $\mathcal{M}$ itself can play the role of the control qubit. Substituting these states into equation (4.18), we have completely recovered the action of the original quantum SWITCH on an initial state $|\varphi\rangle_{\mathcal{S}}$. Later, we will argue that this scheme constitutes a true implementation of the quantum SWITCH supermap.

4.4.2 Via Decaying Atoms

Although a method using time-bin entangled photons has been put forward, it might be objected that the control over this set of states is too exquisite to be practical. Also, it may appear that the scheme depends entirely on time-bin entanglement as a resource. To mitigate these concerns, we show here that one can realise the usual quantum SWITCH using the decays of two unentangled atoms, as previously described. To this end, we have to decouple $\mathcal{M}$ from the other systems. First, if the two atoms are positioned so that the emitted photons enter the machine at different positions, then the machine can record the order in which the two decays took place. The diagram for the scheme is presented in Fig. 4.1, with $V_A^C = H$ and $V_B^C = \sigma_z$.

By inspecting Eqs. (4.16) and (4.17) (or equation (4.13)) for $\chi_{AB}(t_A, t_B) = \chi_A(t_A)\chi_B(t_B)$ with $\chi_A(t) = \chi_B(t)$, we verify that in order to decouple the machine states $|t_A, t_B\rangle_{\mathcal{M}}$ from the system and the control qubit, it is sufficient that $|t_A, t_B\rangle_{\mathcal{M}} = |t_B, t_A\rangle_{\mathcal{M}}$. This is the reason for the beam splitter before the timer in Fig. 4.1. The timer, which represents the state of the machine, records the time of arrival of both photons, but not which one arrived first, because the beam splitter sends both photons to the two detectors $\mathcal{D}_{1\mathcal{T}}$ and $\mathcal{D}_{2\mathcal{T}}$ with equal probability.

As $|t_A, t_B\rangle_{\mathcal{M}} = |t_B, t_A\rangle_{\mathcal{M}}$, we can perform the change of variables $t_A \rightleftharpoons t_B$ in the integral of the state $|1\rangle_{\mathcal{C}'}$ of equation (4.17) (or, similarly, in the second integral of equation (4.13)) to obtain $|\psi\rangle_{\mathcal{C}'\mathcal{S}} = |\psi\rangle_{\mathcal{M}\mathcal{C}\mathcal{S}}$ written as

$$|\psi\rangle_{\mathcal{M}\mathcal{S}\mathcal{C}} = \int_{t_0}^{\infty} dt_A \int_{t_A}^{\infty} dt_B \; \chi(t_A)\chi(t_B) \; |t_A, t_B\rangle_{\mathcal{M}} \otimes \Big[|0\rangle_{\mathcal{C}} \; U_B \; U_A \; |\varphi\rangle_{\mathcal{S}} + |1\rangle_{\mathcal{C}} \; U_A \; U_B \; |\varphi\rangle_{\mathcal{S}} \Big]. \tag{4.20}$$

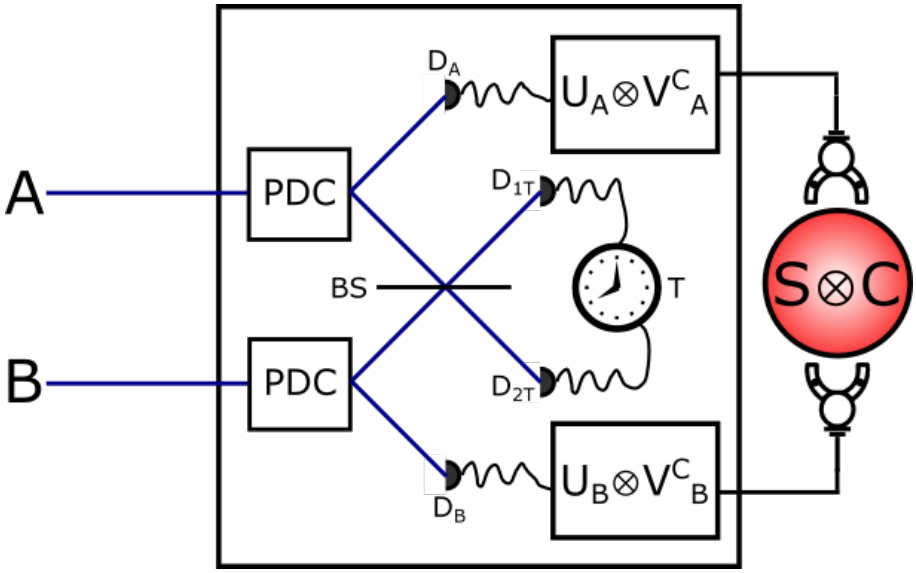


Figure 4.1: Photons from the decays of atoms A and B travel to the machine, which operates on the system and control qubit with the corresponding unitary when a photon is received. A photon enters the machine and undergoes parametric down conversion (PDC), being split into two photons. One of these photons travels to a detector ($\mathcal{D}_A/\mathcal{D}_B$) which triggers the unitary associated with that particular atom on the system ($U_{A/B}$ on $\mathcal{S}$) and the control ($V^C_{A/B}$ on $\mathcal{C}$). The other travels, via a beam splitter (BS), to one of two detectors ($\mathcal{D}_{1\mathcal{T}}$ or $\mathcal{D}_{2\mathcal{T}}$), which cause the timer ($\mathcal{T}$) to record the time of arrival of the photon, but not which photon arrived first.

Now the machine ($\mathcal{M}$) and the rest of the system ($\mathcal{SC}$) are in a product state. We are thus free to discard $\mathcal{M}$. What remains is the desired result — the expression for the quantum SWITCH with a simple two-level control system.

4.4.3 Alternative Derivation for Decaying Atoms protocol

In the derivation of the quantum SWITCH from events which are uncertain in time detailed in section 4.3, the Schrödinger equation is applied in short time slices to the overall state of all of the systems involved in the process. The 'superposition in time' is apparent from the state of the machine which records the time of the triggering events. It might be contended that this implies that the superposition in time is not fundamental for the emergence of the indefinite causal order, but is instead its byproduct. In this section, an alternative derivation is presented, in which the fundamental role of the superposition in time is more explicit. The two derivations are equivalent, but highlight different aspects of the protocol. The

first derivation proceeds in order of temporal priority (the Schrödinger equation is applied step by step in time). This second derivation proceeds in order of logical or causal priority. We derive the states of the relevant systems at the end of the process by considering the correlations that are built up by their interactions.

As in the section above, we consider the situation in which two excited atoms (A and B) are positioned so that the photons associated with their decay will enter the machine at two different positions, as in figure 4.1. Atoms are used as an example, but, as in the first derivation, any process which can give rise to the required superposition can be utilised. If there were a timer which recorded the time of the decay of one of the atoms (or one of the events) then its state after sufficient time has elapsed could in general be written

$$|T\rangle_T = \int_{t_0}^{\infty} dt\ \chi(t)\,|t\rangle_T\,, \tag{4.21}$$

where the states $|t\rangle$ are the orthogonal basis states of the timer associated with the time of the decay. In the case of two events, the state representing their times can similarly be written

$$|T_{AB}\rangle_T = \int_{t_0}^{\infty} dt_A \int_{t_0}^{\infty} dt_B\ \chi(t_A, t_B)\,|t_A, t_B\rangle_T\,. \tag{4.22}$$

In this particular case, the time at which the decays take place are 'recorded' by the photons emitted. So we can make the substitution:

$$|t_i\rangle_T \to a^\dagger_{t_i}\,|0\rangle_\gamma\,. \tag{4.23}$$

The initial state of the total system is the product state

$$|\Psi_0\rangle = |e,e\rangle_{AB}\,|0\rangle_\gamma\,|0,0\rangle_{\mathcal{M}}\,|+\rangle_{\mathcal{C}}\,|\varphi\rangle_{\mathcal{S}}\,, \tag{4.24}$$

where the first ket represents the atoms in their excited states, the second is the vacuum of the photon field, the third represents the state of the machine, and the fourth and fifth are the initial states of the register (control) qubit and the target system respectively. Thus, once the decays take place, the full state becomes

$$|\Psi_1\rangle = \int_{t_0}^{\infty}\int_{t_0}^{\infty} dt_A dt_B\ \chi(t_A,t_B)\,|g,g\rangle_{AB}\,a^\dagger_{t_A}a^\dagger_{t_B}\,|0\rangle_\gamma\,|0,0\rangle_{\mathcal{M}}\,|+\rangle_{\mathcal{C}}\,|\varphi\rangle_{\mathcal{S}}\,, \tag{4.25}$$

where the labels on the photon creation operators denote the time of emission. After the photons are absorbed by the machine, and the machine records the times of arrival and acts on the system and control, the state becomes

$$\begin{aligned}|\Psi_2\rangle = &\int_0^{\infty} dt_A \int_{t_A}^{\infty} dt_B\ \chi(t_A,t_B)\,|g,g\rangle_{AB}\,|0\rangle_\gamma\,|t_A,t_B\rangle_{\mathcal{M}}\,V_B^{\mathrm{C}}V_A^{\mathrm{C}}\,|+\rangle_{\mathcal{C}}\,U_BU_A\,|\varphi\rangle_{\mathcal{S}}\\ &+\int_0^{\infty} dt_B \int_{t_B}^{\infty} dt_A\ \chi(t_A,t_B)\,|g,g\rangle_{AB}\,|0\rangle_\gamma\,|t_A,t_B\rangle_{\mathcal{M}}\,V_A^{\mathrm{C}}V_B^{\mathrm{C}}\,|+\rangle_{\mathcal{C}}\,U_AU_B\,|\varphi\rangle_{\mathcal{S}}\,.\end{aligned} \tag{4.26}$$

The integral has been split into two parts, for the first $t_A < t_B$, and for the second $t_A < t_B$. Again, $|t_A,t_B\rangle_M$ is the state of the machine having operated at times t_A and t_B. As above, we choose $V_A^C = H$ and $V_B^C = \sigma_z$ so that the control qubit will end up in one of the orthogonal states $|0/1\rangle_{\mathcal{C}}$, depending on the order of application of V_A^C and V_B^C.

In order to recover the output of the quantum SWITCH, there is one further requirement. We must decouple the machine and register states from the control and system qubits. As in the previous section, it is sufficient to have machine states $|t_A,t_B\rangle_{\mathcal{M}}$ that are symmetric with respect to a swap in their arguments. That is to say that the mechanisms might record the times at which photons arrived, but not which photon arrived first. This is intuitively expected, since if any information about the order of events is stored in the environment then the entanglement between the control qubit and the target system will be reduced.

Assuming that we prepare our system in such a way that the states $|t_A,t_B\rangle_{\mathcal{M}}$ satisfy this condition, and assuming an analogous symmetry for the probability amplitude χ, by swapping the integration variables in the second integral $(t_A \rightleftharpoons t_B)$ we have:

$$|\Psi_3\rangle = |g,g\rangle_{AB}\,|0\rangle_\gamma \int_0^\infty dt_A \int_{t_A}^\infty dt_B\ \chi(t_A,t_B)\,|t_A,t_B\rangle_{\mathcal{M}} \otimes\Big(\,|0\rangle_{\mathcal{C}}\otimes U_B U_A\,|\varphi\rangle_{\mathcal{S}} + |1\rangle_{\mathcal{C}}\otimes U_A U_B\,|\varphi\rangle_{\mathcal{S}}\,\Big), \tag{4.27}$$

which is the desired product state between the different parts. Tracing out the atoms, photon field and mechanisms for the register and machine systems yields the output of the quantum SWITCH.

4.5 Discussion

This work was motivated in part by the ongoing debate about what constitutes a true implementation of an indefinite causal order, and whether one can be achieved without superpositions of space-time in a quantum gravitational framework. We will now ask whether our quantum SWITCH protocol represents a true ICO and in what respects it is similar and different to other implementations.

A similarity between our scheme and the quantum SWITCHes that have already been implemented in experiments is that they share the same representation in the process matrix formalism. This formalism gives a framework for quantum mechanics in situations where the causal structure is indefinite. The quantum SWITCH has been studied [10] using this formalism, including cases where the operations are performed on time-delocalised subsystems. The process matrix specifies the input and output Hilbert spaces on which the quantum operations taking place during the process act. In our scheme, the nature of the time-delocalisation is explicit — the input and output Hilbert subspaces are given by the Hilbert subspaces associated with each time slice of Fig. 4.2.

Let us consider the spaces on which the operations are performed in the case of the time-bin entangled photons implementation, since there are then only two relevant times, t_e and t_l. At any particular time t, the full Hilbert space of all the relevant systems is given by

$$\mathcal{H}^t_{total} = \mathcal{H}^t_{\mathcal{C}} \otimes \mathcal{H}^t_{\mathcal{S}}. \tag{4.28}$$

The input Hilbert space for operation A is contained within a tensor product of Hilbert spaces associated with the systems at different times

$$\mathcal{H}'_{A_I} = \mathcal{H}_{\mathcal{C}}^{t_{e-}} \otimes \mathcal{H}_{\mathcal{S}}^{t_{e-}} \otimes \mathcal{H}_{\mathcal{C}}^{t_{l-}} \otimes \mathcal{H}_{\mathcal{S}}^{t_{l-}}, \tag{4.29}$$

where the times t_{e-} and t_{l-} denote the moments before the operations are executed at the early and late times respectively. However, the input space itself is a subspace of this larger space. This subspace, $\mathcal{H}_{A_I}$, is a factor of $\mathcal{H}'_{A_I}$, and is defined by the observable algebra generated by the operators

$$O_{A_I} \equiv |0\rangle\langle 0|_{\mathcal{C}} \otimes O_S^{t_{e-}} \otimes \mathbb{I}_S^{t_{l-}} + |1\rangle\langle 1|_{\mathcal{C}} \otimes \mathbb{I}_S^{t_{e-}} \otimes O_S^{t_{l-}}. \tag{4.30}$$

Similarly, the output space for operation A is contained within the product

$$\mathcal{H}'_{A_O} = \mathcal{H}_{\mathcal{C}}^{t_{e+}} \otimes \mathcal{H}_{\mathcal{S}}^{t_{e+}} \otimes \mathcal{H}_{\mathcal{C}}^{t_{l+}} \otimes \mathcal{H}_{\mathcal{S}}^{t_{l+}}, \tag{4.31}$$

where the times t_{e+} and t_{l+} denote the moments after the operations are executed at the early and late times respectively, and is defined by the algebra generated by

$$O_{A_O} \equiv |0\rangle\langle 0|_{\mathcal{C}} \otimes O_S^{t_{e+}} \otimes \mathbb{I}_S^{t_{l+}} + |1\rangle\langle 1|_{\mathcal{C}} \otimes \mathbb{I}_S^{t_{e+}} \otimes O_S^{t_{l+}}. \tag{4.32}$$

The spaces relevant to operation B are identical, except with $|0\rangle\langle 0|_{\mathcal{C}}$ replaced by $|1\rangle\langle 1|_{\mathcal{C}}$ and vice versa. These input and output subspaces are tensor products of Hilbert spaces which are associated with systems at different times, with the correct form for physical realisations of the quantum SWITCH (once the spaces with label t_{e+} are identified with those with label t_{l-}, since no operations are performed between these two times).

It can be seen, therefore, that the process described above is represented by the same process matrix as discussed in Ref. [10], implying that this scheme is a true implementation of the quantum SWITCH. The only difference is that the delocalisation in time of the operations is the fundamental and explicit foundation of this protocol.

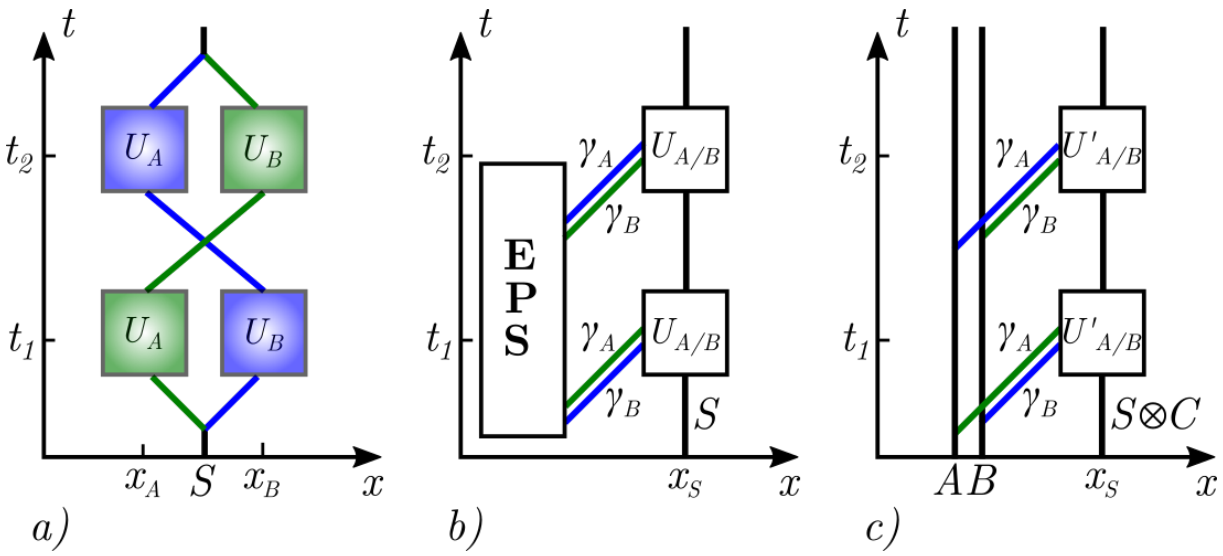


Figure 4.2: Spacetime diagrams for three implementations of the quantum SWITCH a) An implementation using a superposition of spatial trajectories to achieve the SWITCH must have 4 spacetime points associated with the operations. The spatial degree of freedom of the system is in a superposition (green and blue), and so the operations all take place at 4 distinct spacetime points: $[(x_A, t_1),(x_B, t_1),(x_A, t_2),(x_B, t_2)]$. b) and c) show our scheme using time bin entangled photons (EPS) (b) and decaying atoms A and B (c). An implementation using our scheme relies upon superpositions in time, rather that in space, of the events. It is therefore possible to construct a SWITCH in which there are only two spacetime points associated with the operations.

We now comment on the major difference between our scheme and previously implemented protocols. It has been argued [24] that the photonic implementations of the quantum SWITCH are disqualified from being genuine ICOs, because they involve four spacetime events. It is therefore important to address whether our scheme can be criticised in the same way. The two situations are represented in Fig. 4.2. Diagram a) represents schematically implementations that rely on superposition in space, such as the photonic implementations mentioned above. Diagrams b) and c) represent two versions of our protocol, relying on superpositions in time.

From these diagrams, we can see that in Ref. [18], for example, the control qubit is entangled with the spatial degree of freedom of the system. Then, in one branch Alice applies the U_A controlled unitary at spacetime event (t_1, x_A) and Bob applies the controlled unitary U_B at (t_2, x_B), while in the other branch Bob acts at (t_1, x_B) and Alice at (t_2, x_A). Then the system and control are recombined. We therefore see that four spacetime events are relevant to describe the process

that the system undergoes.

In our approach, however, the system is not required to become delocalised in space. The unitaries are performed at the same spatial location. It is not difficult to identify then that there are only two space-time points where the system undergoes a transformation. These are (t_1, x_S) and (t_2, x_S). It has been claimed [24] that this difference in the number of meaningful spacetime points is important for determining whether a true ICO has been achieved. We therefore believe that this protocol really does implement a genuine quantum SWITCH.

This work only considers how the quantum SWITCH might arise as a result of superpositions in time. However, the SWITCH is not the only indefinite causal structure. Further work is needed to discover which other structures can arise in a similar way, and whether there are any allowed causal structures which cannot be realised using superpositions in time.

Since processes that are indefinite in time occur widely in nature, and we have shown how an ICO can arise straightforwardly when such superpositions exist, this work suggests that exotic causal structures might be more widespread than previously thought. This encourages the search for exotic causal structures arising naturally. It is possible that certain natural phenomena might be able to be explained only with reference to such causal structures.

And further, by these, my son, be admonished: of making many books there is no end; and much study is a weariness of the flesh.

—Ecclesiastes 12:12 (KJV)

5 Summary and Further Work

Contents

5.1 Summary of Research Findings 69
5.2 Avenues for Further Investigation 71

5.1 Summary of Research Findings

The focus of this thesis has been the examination of novel properties of indefinite causal orders. The results herein demonstrate new applications for, and new origins of, these phenomena. The author believes that this work adds to the growing body of evidence that indefinite causal orders are an important and fruitful field of research, providing new insights into various fields of Physics.

From its origins at the dawn of the industrial revolution, the study of thermodynamics has been based upon principles derived from machines which operate in a cycle with a predetermined causal ordering. The author has outlined the first thermodynamic cycle which operates in a quantum superposition of orders. It was shown that operations which by themselves are useless for thermodynamic tasks when applied in any fixed causal order, can be 'activated' and become useful for performing such tasks. In particular, a protocol for refrigeration, which uses

thermalising channels in an indefinite causal order controlled by the quantum SWITCH, was developed. This refrigerator is the first to rely on indefinite causal orders. It shares some similarity with 'Maxwell's Demon'-like quantum heat engines, such as the Szilard engine [59], since the cost of its operation comes from the erasure of information. This first application of ICOs to thermodynamics opens up an entirely new arena for their application. Additionally, applying the formalisms of thermodynamics to indefinite causal orders will open up new knowledge about the physics underlying them.

In the third chapter of this thesis, the first simulation of indefinite causal order on a programmable quantum computer was presented, using cloud quantum computing resources available to all users of the internet. The refrigeration protocol of the preceding chapter was adapted so that it could be implemented using IBM's superconducting transmon qubit processors. As far as the author is aware, this also represents the first refrigeration cycle to be run on a programmable quantum computer. The fact that this is possible demonstrates that current quantum computing technology provides an excellent test bed for protocols involving ICOs and thermodynamic protocols in general. It also demonstrates the robustness of the refrigeration cycle to noise, motivating more investigation into ICO protocols using NISQ era devices.

Lastly, a new context for the generation of indefinite causal orders was put forward. It was shown that processes which have a quantum uncertainty associated with their timing can be exploited in such a way as to give rise to ICOs. The various disagreements about the validity of physical realisations of quantum causal orders were discussed, and it was argued that the scheme constitutes a genuine ICO, on the grounds that it shares the correct process matrix and has only two relevant spacetime points. The fact that ICOs can arise from phenomena that are so common in nature indicates that they might be much more widespread than has previously been imagined, and so are an important subject for further study.

5.2 Avenues for Further Investigation

The ICO refrigerator detailed in this thesis is only the first thermodynamic protocol to use exotic causal structures. This work paves the way for further investigation and development of new procedures — it is reasonable to assume that there will be many other examples which are discovered over the coming years. An obvious next step would be the development of a heat engine which uses quantum causality for its operation. Another open question is whether the efficiency of the refrigeration cycle proposed can be improved. The author believes that this should be possible, by replacing certain irreversible classical steps of the protocol with reversible ones, for instance. In principle, there seems to be no reason why the efficiency of a cycle based on ICOs should not approach the Carnot efficiency. If it was discovered that this was impossible then this would be a surprising result, and would raise an interesting question about the thermodynamic properties of quantum causal orders. The potential for thermalising channels alone to execute refrigeration, when these channels are allowed to be performed in a superpostion of causal orders, suggests that a thermodynamic resource theory which included ICOs would have very different properties from one in which the causal order was fixed. The set of achievable tasks, given a set of free operations, is different in at least this one case, and it is reasonable to assume that there are other examples. Formalising such a resource theory would be a very promising avenue for further work.

Quantum computers offer an excellent method for the exploration of the properties of diverse kinds of ICO protocols. Any channel can be chosen for placement in a simulated quantum SWITCH, and the SWITCH itself can be generalised for the placing of three or more channels in a quantum causal order. The versatile nature of the programmable computers provided by IBM makes the adaptation and testing of different procedures very efficient. Several concrete proposals were put forward in chapter 3 — fuller simulations of the quantum fridge which might help further assessment of the protocol's suitability for different applications. More broadly, this new context for testing ICO protocols should

encourage further probing for the limitations of the quantum SWITCH in assisting thermodynamic and other types of tasks.

The fact that superpositions in time, when configured in a suitable way, can give rise to the quantum SWITCH, suggests that it might be possible to produce other causal structures in a similar way. This possibility is yet to be explored. To take a simple example: by simply adding more triggering events (i.e. more atoms), higher order quantum SWITCHes could, of course, be constructed.

In addition, several simplifying assumptions were made in the construction of the quantum SWITCH from time superpositions. It is possible that by considering more general cases, new ICO protocols could be constructed which might have different properties than those which have already been proposed. For example, it was assumed that in the time between triggering events, the system does not evolve - if this assumption was relaxed, in the case of a continuous probability distribution for the events (i.e. decaying atoms), then a continuous superposition of different states would arise, corresponding to the times of the second decay. By then making a measurement of the times in a suitable basis, it might be possible to use the interference between these states in a constructive way. Another assumption was that the operations were performed instantaneously, and thus there could be no overlap between their times. Relaxing this assumption would also lead to some non-trivial, and perhaps useful, superposition. Lastly, we did not discuss the case where the events which are used to trigger the operations are themselves entangled so that there are interesting correlations between their times.

Finally, investigations into quantum causal orders were first motivated by discussions concerning quantum gravity [4]. Perhaps, by considering how these structures can arise from the simplest phenomena, it might be possible to shed some light on this difficult subject.

Appendices

A

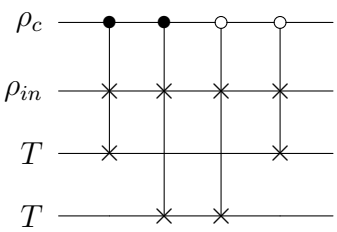
Supplementary Materials - Cloud Quantum Refrigerator

Contents

A.1 Quantum Circuit Output Calculation 75
A.2 IBMq Transpiled Circuit 78

A.1 Quantum Circuit Output Calculation

Here the output of the simulation circuit implemented in chapter 3 is calculated, in order to verify that that this circuit generates the correct output. We reproduce this circuit below for ease of reference.



Recall that the initial state of the control qubit $\rho_c = |\psi_c\rangle\langle\psi_c|$, where $|\psi_c\rangle = \sqrt{\alpha}\,|0\rangle + \sqrt{1-\alpha}\,|1\rangle$. We can then write the output of the circuit as a sum over

the matrix elements of ρ_c.

$$\begin{aligned}\rho_{total}^{out} = \alpha\,|0\rangle\langle 0| \otimes S_2S_1\Big(\rho_{in}\otimes T\otimes T\Big)S_1^\dagger S_2^\dagger \\ +\sqrt{\alpha(1-\alpha)}\,|0\rangle\langle 1| \otimes S_2S_1\Big(\rho_{in}\otimes T\otimes T\Big)S_2^\dagger S_1^\dagger \\ +\sqrt{\alpha(1-\alpha)}\,|1\rangle\langle 0| \otimes S_1S_2\Big(\rho_{in}\otimes T\otimes T\Big)S_1^\dagger S_2^\dagger \\ +(1-\alpha)\,|1\rangle\langle 1| \otimes S_1S_2\Big(\rho_{in}\otimes T\otimes T\Big)S_2^\dagger S_1^\dagger,\end{aligned} \tag{A.1}$$

where the tensor product proceeds in descending order along the qubits in the circuit and S_1 and S_2 are the unitaries representing swaps between the second and third qubits, and the second and fourth qubits, respectively. Note that, on each line, only two unitaries act from each side. This is because, for each basis state of the control qubit, there are two gates which do not act.

We now expand the density operators for ρ_{in} and T in terms of the computational basis states.

$$\begin{aligned}\rho_{in} &\equiv \sum_{ij} r_{ij}\,|i\rangle\langle j| \\ T &\equiv \sum_k q_k\,|k\rangle\langle k|\,.\end{aligned} \tag{A.2}$$

The form of ρ_{in} is kept general, but T must be diagonal. Let us now consider the action of the swapping unitaries on the states of the bottom three qubits. For the control qubit state $|0\rangle$, S_1 acts first and then S_2.

$$\begin{aligned}&|0\rangle \otimes S_2S_1\Big(\,|i\rangle\otimes|k\rangle\otimes|m\rangle\,\Big) \\ =&\,|0\rangle \otimes S_2\Big(\,|k\rangle\otimes|i\rangle\otimes|m\rangle\,\Big) \\ =&\,|0\rangle\otimes|m\rangle\otimes|i\rangle\otimes|k\rangle\,.\end{aligned} \tag{A.3}$$

For the control qubit state $|1\rangle$, S_2 acts first and then S_1.

$$\begin{aligned}&|1\rangle \otimes S_1S_2\Big(\,|i\rangle\otimes|k\rangle\otimes|m\rangle\,\Big) \\ =&\,|1\rangle \otimes S_1\Big(\,|m\rangle\otimes|k\rangle\otimes|i\rangle\,\Big) \\ =&\,|1\rangle\otimes|k\rangle\otimes|m\rangle\otimes|i\rangle\,.\end{aligned} \tag{A.4}$$

It is now possible to rewrite equation A.1:

$$\begin{aligned}\rho_{total}^{out} = \sum_{ijkm} r_{ij}q_k q_m \Big[& \alpha \left|0\right\rangle \left\langle 0\right| \otimes \left|m\right\rangle \left\langle m\right| \otimes \left|i\right\rangle \left\langle j\right| \otimes \left|k\right\rangle \left\langle k\right| \\ & + \sqrt{\alpha(1-\alpha)} \left|0\right\rangle \left\langle 1\right| \otimes \left|m\right\rangle \left\langle k\right| \otimes \left|i\right\rangle \left\langle m\right| \otimes \left|k\right\rangle \left\langle j\right| \\ & + \sqrt{\alpha(1-\alpha)} \left|1\right\rangle \left\langle 0\right| \otimes \left|k\right\rangle \left\langle m\right| \otimes \left|m\right\rangle \left\langle j\right| \otimes \left|i\right\rangle \left\langle k\right| \\ & + (1-\alpha) \left|1\right\rangle \left\langle 1\right| \otimes \left|k\right\rangle \left\langle k\right| \otimes \left|m\right\rangle \left\langle m\right| \otimes \left|i\right\rangle \left\langle j\right| \Big]. \end{aligned} \tag{A.5}$$

We proceed to trace out the reservoir qubits in order to recover the quantum channel which acts on the control and system qubits. Let us each of the four terms in this expression. The diagonal (first and last) terms, reduce simply:

$$\sum_{ijkm} r_{ij}q_k q_m \left|0\right\rangle \left\langle 0\right| \otimes \left|m\right\rangle \left\langle m\right| \otimes \left|i\right\rangle \left\langle j\right| \otimes \left|k\right\rangle \left\langle k\right| \rightarrow \left|0\right\rangle \left\langle 0\right| \otimes \sum_m q_m \left|m\right\rangle \left\langle m\right|, \tag{A.6}$$

and

$$\sum_{ijkm} r_{ij}q_k q_m \left|1\right\rangle \left\langle 1\right| \otimes \left|k\right\rangle \left\langle k\right| \otimes \left|m\right\rangle \left\langle m\right| \otimes \left|i\right\rangle \left\langle j\right| \rightarrow \left|1\right\rangle \left\langle 1\right| \otimes \sum_k q_k \left|k\right\rangle \left\langle k\right|. \tag{A.7}$$

The off-diagonal terms are slightly more complicated. We consider initially the term with control qubit factor $\left|0\right\rangle \left\langle 1\right|$. First we trace out the fourth qubit.

$$\begin{aligned} & \sum_{ijkm} r_{ij}q_k q_m \left|0\right\rangle \left\langle 1\right| \otimes \left|m\right\rangle \left\langle k\right| \otimes \left|i\right\rangle \left\langle m\right| \otimes \left|k\right\rangle \left\langle j\right| \\ & \rightarrow \sum_{ijkmp} r_{ij}q_k q_m \left\langle p|k\right\rangle \left\langle j|p\right\rangle \left|0\right\rangle \left\langle 1\right| \otimes \left|m\right\rangle \left\langle k\right| \otimes \left|i\right\rangle \left\langle m\right| \\ & = \sum_{ijkmp} r_{ij}q_k q_m \delta_{pk}\delta_{jp} \left|0\right\rangle \left\langle 1\right| \otimes \left|m\right\rangle \left\langle k\right| \otimes \left|i\right\rangle \left\langle m\right| \\ & = \sum_{ijm} r_{ij}q_j q_m \left|0\right\rangle \left\langle 1\right| \otimes \left|m\right\rangle \left\langle j\right| \otimes \left|i\right\rangle \left\langle m\right|. \end{aligned} \tag{A.8}$$

Next the third qubit is traced out.

$$\begin{aligned} & \sum_{ijm} r_{ij}q_j q_m \left|0\right\rangle \left\langle 1\right| \otimes \left|m\right\rangle \left\langle j\right| \otimes \left|i\right\rangle \left\langle m\right| \\ & \rightarrow \sum_{ijms} r_{ij}q_j q_m \left\langle s|i\right\rangle \left\langle m|s\right\rangle \left|0\right\rangle \left\langle 1\right| \otimes \left|m\right\rangle \left\langle j\right| \\ & = \sum_{ijms} r_{ij}q_j q_m \delta_{si}\delta_{ms} \left|0\right\rangle \left\langle 1\right| \otimes \left|m\right\rangle \left\langle j\right| \\ & = \sum_{ijms} r_{ij}q_i q_j \left|0\right\rangle \left\langle 1\right| \otimes \left|i\right\rangle \left\langle j\right|. \end{aligned} \tag{A.9}$$

The final term with control qubit factor $|1\rangle\langle 0|$ reduces similarly:

$$\sum_{ijkm} r_{ij}q_k q_m \,|1\rangle\langle 0| \otimes |k\rangle\langle m| \otimes |m\rangle\langle j| \otimes |i\rangle\langle k| \to \sum_{ij} r_{ij}q_i q_j \,|0\rangle\langle 1| \otimes |i\rangle\langle j|\,. \quad \text{(A.10)}$$

By recombining these four terms and recalling the definitions of equation (A.2), we see that the output marginal state of the control and system qubits is given by

$$\begin{aligned}\rho_{1,2}^{out} = &\Big(\alpha\,|0\rangle\langle 0| + (1-\alpha)\,|1\rangle\langle 1|\Big) \otimes T \\ &+ \sqrt{\alpha(1-\alpha)}\Big(\,|0\rangle\langle 1| + |1\rangle\langle 0|\,\Big) \otimes T\rho_{in}T. \end{aligned} \quad \text{(A.11)}$$

Here, the subscript of ρ^{out} denotes the qubits which remain after the tracing-out process. This expression is identical to that for the quantum SWITCH of thermalising channels $S(\mathcal{N}^T, \mathcal{N}^T)(\rho_c \otimes \rho_{in})$ derived in equation (2.4), therefore we conclude that the circuit gives the correct output.

One further consideration is the marginal output state of the reservoir qubits. Of particular interest is the effective temperature of each reservoir qubit after the circuit has been implemented. Starting again from equation (A.5), we instead trace out all but the first and last qubit to give:

$$\begin{aligned}\rho_{1,4}^{out} = &\,\alpha\,|0\rangle\langle 0| \otimes \sum_k q_k\,|k\rangle\langle k| \\ &+\sqrt{\alpha(1-\alpha)}\,|0\rangle\langle 1| \otimes \sum_{ij} r_{ij}q_i^2\,|i\rangle\langle j| \\ &+\sqrt{\alpha(1-\alpha)}\,|1\rangle\langle 0| \otimes \sum_{ij} r_{ij}q_j^2\,|i\rangle\langle j| \\ &+(1-\alpha)\,|1\rangle\langle 1| \otimes \sum_k q_k\,|k\rangle\langle k|\,. \end{aligned} \quad \text{(A.12)}$$

In the case where ρ_{in} is diagonal (i.e. $r_{ij} = \delta_{ij}r_{ii}$), then this is identical to equation (A.11), implying that the marginal output effective temperatures are the same for the work (second) qubit and the reservoir (thrid and fourth) qubits. This is the case considered in chapter 3.

A.2 IBMq Transpiled Circuit

The circuit which is given as input to the IBMq transpiler is reproduced in figure A.1. The controlled swaps are represented by a combination of Toffoli and controlled-not gates.

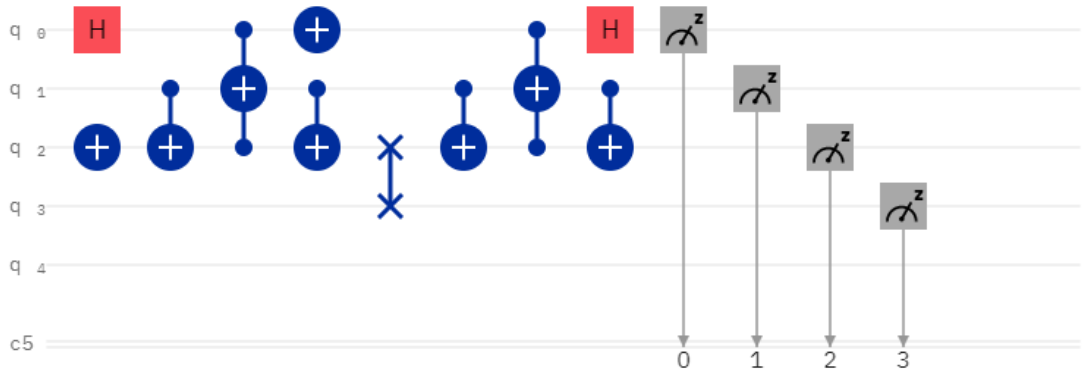


Figure A.1: The input circuit for a particular input computational basis state (in this case work qubit (q_2) '1', reservoir A (q_1) '0' and reservoir B (q_3) '0'). H labels Hadamard gates, + not gates, and the first operation involving q_3 is a swap gate. The final four operations are measurements, with the results stored in a classical register.

This circuit must be executed using a quantum processor that does not have full connectivity, and cannot natively perform Toffoli gates. It is therefore transpiled into a form which is compatible with the processor architecture. This transpiling is carried out automatically when a job is sent to the IBMq servers. The resulting circuit is given below:

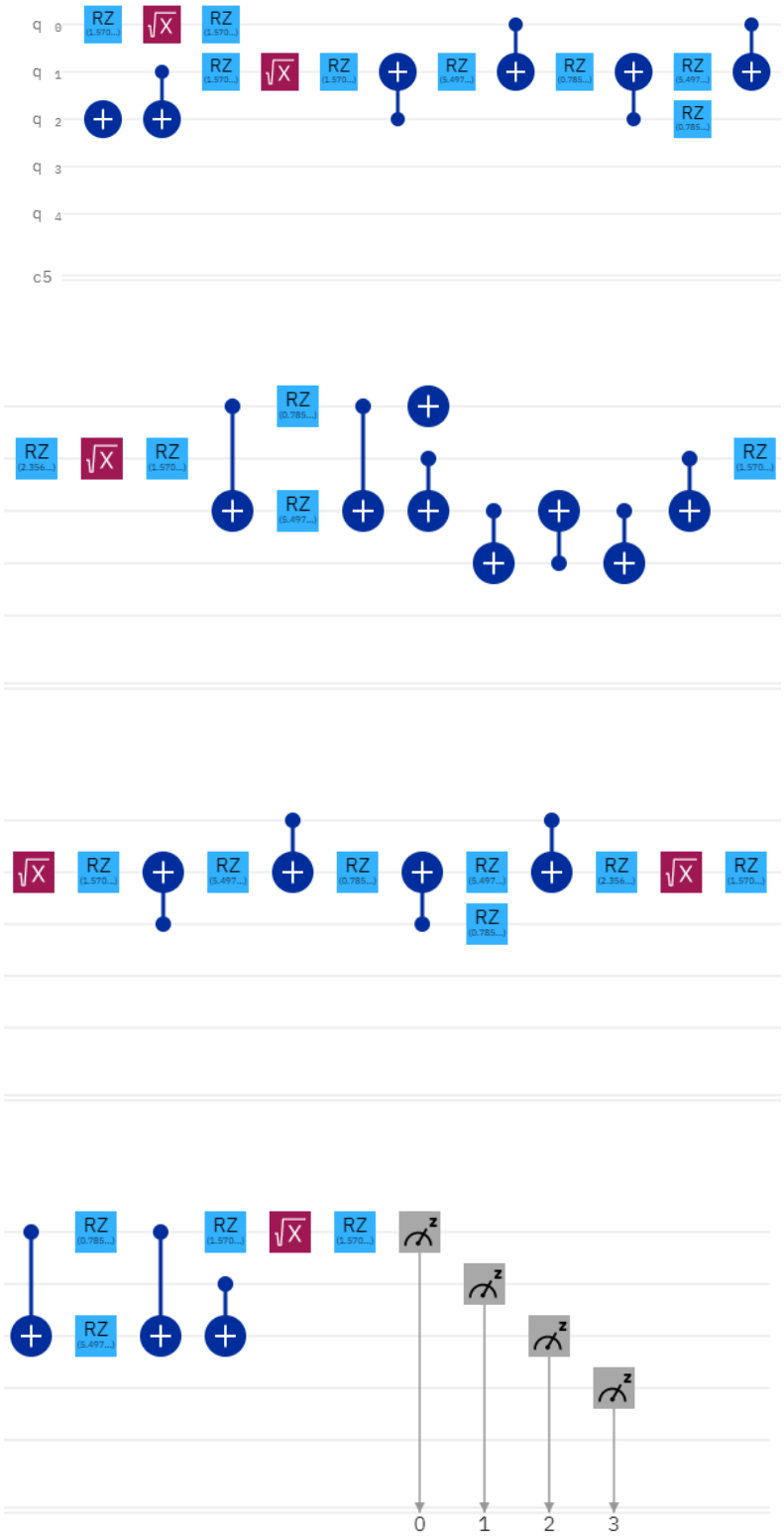


Figure A.2: Transpiled circuit (for the input in figure A.1) which is executed by the Yorktown quantum processor. The circuit is divided between two lines for readability. RZ labels rotation around the z-axis in the Bloch sphere.

The Qiskit code for this circuit, which can be run directly using IBMq, is reproduced here for reference and to provide numerical values for gate rotations:

```
from qiskit import QuantumRegister, ClassicalRegister, QuantumCircuit
from numpy import pi

qreg_q = QuantumRegister(5, 'q')
creg_c = ClassicalRegister(5, 'c')
circuit = QuantumCircuit(qreg_q, creg_c)

circuit.rz(1.5707963267948961, qreg_q[0])
circuit.sx(qreg_q[0])
circuit.rz(1.5707963267948966, qreg_q[0])
circuit.x(qreg_q[2])
circuit.cx(qreg_q[1], qreg_q[2])
circuit.rz(1.5707963267948961, qreg_q[1])
circuit.sx(qreg_q[1])
circuit.rz(1.5707963267948966, qreg_q[1])
circuit.cx(qreg_q[2], qreg_q[1])
circuit.rz(5.497787143782137, qreg_q[1])
circuit.cx(qreg_q[0], qreg_q[1])
circuit.rz(0.7853981633974487, qreg_q[1])
circuit.cx(qreg_q[2], qreg_q[1])
circuit.rz(5.497787143782137, qreg_q[1])
circuit.cx(qreg_q[0], qreg_q[1])
circuit.rz(2.356194490192344, qreg_q[1])
circuit.sx(qreg_q[1])
circuit.rz(1.5707963267948966, qreg_q[1])
circuit.rz(0.7853981633974487, qreg_q[2])
circuit.cx(qreg_q[0], qreg_q[2])
circuit.rz(0.7853981633974487, qreg_q[0])
circuit.rz(5.497787143782137, qreg_q[2])
circuit.cx(qreg_q[0], qreg_q[2])
circuit.x(qreg_q[0])
circuit.cx(qreg_q[1], qreg_q[2])
circuit.cx(qreg_q[2], qreg_q[3])
circuit.cx(qreg_q[3], qreg_q[2])
circuit.cx(qreg_q[2], qreg_q[3])
circuit.cx(qreg_q[1], qreg_q[2])
circuit.rz(1.5707963267948961, qreg_q[1])
circuit.sx(qreg_q[1])
circuit.rz(1.5707963267948966, qreg_q[1])
circuit.cx(qreg_q[2], qreg_q[1])
circuit.rz(5.497787143782137, qreg_q[1])
circuit.cx(qreg_q[0], qreg_q[1])
circuit.rz(0.7853981633974487, qreg_q[1])
circuit.cx(qreg_q[2], qreg_q[1])
circuit.rz(5.497787143782137, qreg_q[1])
```

```
circuit.cx(qreg_q[0], qreg_q[1])
circuit.rz(2.356194490192344, qreg_q[1])
circuit.sx(qreg_q[1])
circuit.rz(1.5707963267948966, qreg_q[1])
circuit.rz(0.7853981633974487, qreg_q[2])
circuit.cx(qreg_q[0], qreg_q[2])
circuit.rz(0.7853981633974487, qreg_q[0])
circuit.rz(5.497787143782137, qreg_q[2])
circuit.cx(qreg_q[0], qreg_q[2])
circuit.rz(1.5707963267948961, qreg_q[0])
circuit.sx(qreg_q[0])
circuit.rz(1.5707963267948966, qreg_q[0])
circuit.cx(qreg_q[1], qreg_q[2])
circuit.measure(qreg_q[0], creg_c[0])
circuit.measure(qreg_q[1], creg_c[1])
circuit.measure(qreg_q[2], creg_c[2])
circuit.measure(qreg_q[3], creg_c[3])
```

References

[1] E. Schrödinger. "An Undulatory Theory of the Mechanics of Atoms and Molecules". In: *Phys. Rev.* 28 (6 Dec. 1926), pp. 1049–1070. URL: https://link.aps.org/doi/10.1103/PhysRev.28.1049.

[2] M A Nielsen and I L Chuang. *Quantum Computation and Quantum Information*. New York, USA: Cambridge University Press, 2000, p. 360.

[3] Vern Paulsen. *Completely bounded maps and operator algebras*. 78. Cambridge University Press, 2002.

[4] Lucien Hardy. "Towards quantum gravity: a framework for probabilistic theories with non-fixed causal structure". In: *Journal of Physics A: Mathematical and Theoretical* 40.12 (Mar. 2007), pp. 3081–3099. URL: https://doi.org/10.1088%2F1751-8113%2F40%2F12%2Fs12.

[5] Ognyan Oreshkov, Fabio Costa, and Časlav Brukner. "Quantum correlations with no causal order". In: *Nature Communications* 3.1 (Jan. 2012). URL: https://doi.org/10.1038/ncomms2076.

[6] Giulio Chiribella et al. "Quantum computations without definite causal structure". In: *Phys. Rev. A* 88 (2 Aug. 2013), p. 022318. URL: https://link.aps.org/doi/10.1103/PhysRevA.88.022318.

[7] Jean-Philippe W. MacLean et al. "Quantum-coherent mixtures of causal relations". In: *Nature Communications* 8.1 (May 2017). URL: https://doi.org/10.1038/ncomms15149.

[8] Flaminia Giacomini, Esteban Castro-Ruiz, and Časlav Brukner. "Indefinite causal structures for continuous-variable systems". In: *New Journal of Physics* 18.11 (Nov. 2016), p. 113026. URL: https://doi.org/10.1088/1367-2630/18/11/113026.

[9] Mateus Araújo et al. "Witnessing causal nonseparability". In: *New Journal of Physics* 17.10 (Oct. 2015), p. 102001. URL: https://doi.org/10.1088/1367-2630/17/10/102001.

[10] Ognyan Oreshkov. "Time-delocalized quantum subsystems and operations: on the existence of processes with indefinite causal structure in quantum mechanics". In: *Quantum* 3 (Dec. 2019), p. 206. URL: https://doi.org/10.22331/q-2019-12-02-206.

[11] A. Jamiołkowski. "Linear transformations which preserve trace and positive semidefiniteness of operators". In: *Reports on Mathematical Physics* 3.4 (Dec. 1972), pp. 275–278. URL: https://doi.org/10.1016/0034-4877(72)90011-0.

[12] Man-Duen Choi. "Completely positive linear maps on complex matrices". In: *Linear Algebra and its Applications* 10.3 (June 1975), pp. 285–290. URL: https://doi.org/10.1016/0024-3795(75)90075-0.

[13] J. S. Bell. "On the Einstein Podolsky Rosen paradox". In: *Physics Physique Fizika* 1 (3 Nov. 1964), pp. 195–200. URL: https://link.aps.org/doi/10.1103/PhysicsPhysiqueFizika.1.195.

[14] Mateus Araújo et al. "A purification postulate for quantum mechanics with indefinite causal order". In: *Quantum* 1 (Apr. 2017), p. 10. URL: https://doi.org/10.22331/q-2017-04-26-10.

[15] Magdalena Zych et al. "Bell's theorem for temporal order". In: *Nature Communications* 10.1 (Aug. 2019). URL: https://doi.org/10.1038/s41467-019-11579-x.

[16] Lorenzo M. Procopio et al. "Experimental superposition of orders of quantum gates". In: *Nature Communications* 6.1 (Aug. 2015). URL: https://doi.org/10.1038/ncomms8913.

[17] Giulia Rubino et al. "Experimental verification of an indefinite causal order". In: *Science Advances* 3.3 (Mar. 2017), e1602589. URL: https://doi.org/10.1126/sciadv.1602589.

[18] K. Goswami et al. "Indefinite Causal Order in a Quantum Switch". In: *Phys. Rev. Lett.* 121 (9 Aug. 2018), p. 090503. URL: https://link.aps.org/doi/10.1103/PhysRevLett.121.090503.

[19] Kejin Wei et al. "Experimental Quantum Switching for Exponentially Superior Quantum Communication Complexity". In: *Phys. Rev. Lett.* 122 (12 Mar. 2019), p. 120504. URL: https://link.aps.org/doi/10.1103/PhysRevLett.122.120504.

[20] Yu Guo et al. "Experimental Transmission of Quantum Information Using a Superposition of Causal Orders". In: *Phys. Rev. Lett.* 124 (3 Jan. 2020), p. 030502. URL: https://link.aps.org/doi/10.1103/PhysRevLett.124.030502.

[21] K. Goswami et al. "Increasing communication capacity via superposition of order". In: *Phys. Rev. Research* 2 (3 Aug. 2020), p. 033292. URL: https://link.aps.org/doi/10.1103/PhysRevResearch.2.033292.

[22] Giulia Rubino et al. *Experimental Entanglement of Temporal Orders*. 2020. arXiv: 1712.06884 [quant-ph].

[23] Xinfang Nie et al. *Experimental Realization of a Quantum Refrigerator Driven by Indefinite Causal Orders*. 2020. arXiv: 2011.12580 [quant-ph].

[24] Nikola Paunković and Marko Vojinović. "Causal orders, quantum circuits and spacetime: distinguishing between definite and superposed causal orders". In: *Quantum* 4 (May 2020), p. 275. URL: https://doi.org/10.22331/q-2020-05-28-275.

[25] Giulio Chiribella. "Perfect discrimination of no-signalling channels via quantum superposition of causal structures". In: *Phys. Rev. A* 86 (4 Oct. 2012), 040301(R). URL: https://link.aps.org/doi/10.1103/PhysRevA.86.040301.

[26] Timoteo Colnaghi et al. "Quantum computation with programmable connections between gates". In: *Physics Letters A* 376.45 (Oct. 2012), pp. 2940–2943. URL: https://doi.org/10.1016/j.physleta.2012.08.028.

[27] Mateus Araújo, Fabio Costa, and Časlav Brukner. "Computational Advantage from Quantum-Controlled Ordering of Gates". In: *Phys. Rev. Lett.* 113 (25 Dec. 2014), p. 250402. URL: https://link.aps.org/doi/10.1103/PhysRevLett.113.250402.

[28] Daniel Ebler, Sina Salek, and Giulio Chiribella. "Enhanced Communication with the Assistance of Indefinite Causal Order". In: *Phys. Rev. Lett.* 120 (12 Mar. 2018), p. 120502. URL: https://link.aps.org/doi/10.1103/PhysRevLett.120.120502.

[29] Sina Salek, Daniel Ebler, and Giulio Chiribella. *Quantum communication in a superposition of causal orders*. 2018. arXiv: 1809.06655 [quant-ph].

[30] Giulio Chiribella et al. "Indefinite causal order enables perfect quantum communication with zero capacity channels". In: *New Journal of Physics* 23.3 (Mar. 2021), p. 033039. URL: https://doi.org/10.1088/1367-2630/abe7a0.

[31] Chiranjib Mukhopadhyay, Manish K. Gupta, and Arun Kumar Pati. *Superposition of causal order as a metrological resource for quantum thermometry*. 2018. arXiv: 1812.07508 [quant-ph].

[32] Michael Frey. "Indefinite causal order aids quantum depolarizing channel identification". In: *Quantum Inf. Process.* 18.4 (2019), p. 96. URL: https://doi.org/10.1007/s11128-019-2186-9.

[33] Xiaobin Zhao, Yuxiang Yang, and Giulio Chiribella. "Quantum Metrology with Indefinite Causal Order". In: *Phys. Rev. Lett.* 124 (19 May 2020), p. 190503. URL: https://link.aps.org/doi/10.1103/PhysRevLett.124.190503.

[34] David Felce and Vlatko Vedral. "Quantum Refrigeration with Indefinite Causal Order". In: *Phys. Rev. Lett.* 125 (7 Aug. 2020), p. 070603. URL: https://link.aps.org/doi/10.1103/PhysRevLett.125.070603.

[35] Kais Abdelkhalek, Yoshifumi Nakata, and David Reeb. *Fundamental energy cost for quantum measurement*. 2016. arXiv: 1609.06981 [quant-ph].

[36] R. Landauer. "Irreversibility and Heat Generation in the Computing Process". In: *IBM Journal of Research and Development* 5.3 (July 1961), pp. 183–191. URL: https://doi.org/10.1147/rd.53.0183.

[37] Joseph F. Fitzsimons, Jonathan A. Jones, and Vlatko Vedral. "Quantum correlations which imply causation". In: *Scientific Reports* 5.1 (Dec. 2015). URL: https://doi.org/10.1038/srep18281.

[38] David Felce, Vlatko Vedral, and Felix Tennie. *Refrigeration with Indefinite Causal Orders on a Cloud Quantum Computer*. 2021. arXiv: 2107.12413 [quant-ph].

[39] Huan Cao et al. *Experimental demonstration of indefinite causal order induced quantum heat extraction*. 2021. arXiv: 2101.07979 [quant-ph].

[40] *IBM Quantum Experience*. URL: https://quantum-computing.ibm.com/.

[41] Simon J. Devitt. "Performing quantum computing experiments in the cloud". In: *Phys. Rev. A* 94 (3 Sept. 2016), p. 032329. URL: https://link.aps.org/doi/10.1103/PhysRevA.94.032329.

[42] Run-hua Shi et al. "Secure Multiparty Quantum Computation for Summation and Multiplication". In: *Scientific Reports* 6.1 (Jan. 2016). URL: https://doi.org/10.1038/srep19655.

[43] Mario Berta, Stephanie Wehner, and Mark M Wilde. "Entropic uncertainty and measurement reversibility". In: *New Journal of Physics* 18.7 (July 2016), p. 073004. URL: https://doi.org/10.1088/1367-2630/18/7/073004.

[44] Maika Takita et al. "Demonstration of Weight-Four Parity Measurements in the Surface Code Architecture". In: *Phys. Rev. Lett.* 117 (21 Nov. 2016), p. 210505. URL: https://link.aps.org/doi/10.1103/PhysRevLett.117.210505.

[45] Mitali Sisodia, Abhishek Shukla, and Anirban Pathak. "Experimental realization of nondestructive discrimination of Bell states using a five-qubit quantum computer". In: *Physics Letters A* 381.46 (Dec. 2017), pp. 3860–3874. URL: https://doi.org/10.1016/j.physleta.2017.09.050.

[46] Rui Li et al. "Approximate Quantum Adders with Genetic Algorithms: An IBM Quantum Experience". In: *Quantum Measurements and Quantum Metrology* 4.1 (July 2017), pp. 1–7. URL: https://doi.org/10.1515/qmetro-2017-0001.

[47] M. Hebenstreit et al. "Compressed quantum computation using a remote five-qubit quantum computer". In: *Phys. Rev. A* 95 (5 May 2017), p. 052339. URL: https://link.aps.org/doi/10.1103/PhysRevA.95.052339.

[48] R. P. Rundle et al. "Simple procedure for phase-space measurement and entanglement validation". In: *Phys. Rev. A* 96 (2 Aug. 2017), p. 022117. URL: https://link.aps.org/doi/10.1103/PhysRevA.96.022117.

[49] Shi-Yuan Ma et al. "Chiral Spin Flipping Gate Implemented in IBM Quantum Experience". In: *Applied Mathematics & Information Sciences* 11.5 (Sept. 2017), pp. 1519–1526. URL: https://doi.org/10.18576/amis/110531.

[50] Jens Koch et al. "Charge-insensitive qubit design derived from the Cooper pair box". In: *Phys. Rev. A* 76 (4 Oct. 2007), p. 042319. URL: https://link.aps.org/doi/10.1103/PhysRevA.76.042319.

[51] J. A. Schreier et al. "Suppressing charge noise decoherence in superconducting charge qubits". In: *Phys. Rev. B* 77 (18 May 2008), p. 180502. URL: https://link.aps.org/doi/10.1103/PhysRevB.77.180502.

[52] David Felce et al. *Indefinite Causal Orders from Superpositions in Time*. 2021. arXiv: 2107.08076 [quant-ph].

[53] Eduardo O. Dias. "Quantum formalism for events and how time can emerge from its foundations". In: *Phys. Rev. A* 103 (1 Jan. 2021), p. 012219. URL: https://link.aps.org/doi/10.1103/PhysRevA.103.012219.

[54] H. Salecker and E. P. Wigner. "Quantum Limitations of the Measurement of Space-Time Distances". In: *Phys. Rev.* 109 (2 Jan. 1958), pp. 571–577. URL: https://link.aps.org/doi/10.1103/PhysRev.109.571.

[55] Asher Peres. "Measurement of time by quantum clocks". In: *American Journal of Physics* 48.7 (July 1980), pp. 552–557. URL: https://doi.org/10.1119/1.12061.

[56] Don N. Page and William K. Wootters. "Evolution without evolution: Dynamics described by stationary observables". In: *Phys. Rev. D* 27 (12 June 1983), pp. 2885–2892. URL: https://link.aps.org/doi/10.1103/PhysRevD.27.2885.

[57] Harishankar Jayakumar et al. "Time-bin entangled photons from a quantum dot". In: *Nature Communications* 5, 4251 (June 2014), p. 4251. arXiv: 1305.2081 [quant-ph].

[58] Marijn A. M. Versteegh et al. “Single pairs of time-bin-entangled photons”. In: *Phys. Rev. A* 92 (3 Sept. 2015), p. 033802. URL: https://link.aps.org/doi/10.1103/PhysRevA.92.033802.

[59] L. Szilard. “Über die Entropieverminderung in einem thermodynamischen System bei Eingriffen intelligenter Wesen”. In: *Zeitschrift für Physik* 53.11-12 (Nov. 1929), pp. 840–856. URL: https://doi.org/10.1007/bf01341281.